2016•2017
FACULTY OF MEDICINE AND LIFE SCIENCES
Master of Biomedical Sciences

Master's thesis

Investigation of the biological effects of ionizing radiation and iodine deficiency on non-cancerous thyrocytes

Supervisor :
Prof. dr. Niels HELLINGS

Supervisor :
Dr.ir. HANANE DERRADJI

Bertrand Nyuykonge
Thesis presented in fulfillment of the requirements for the degree of Master of Biomedical Sciences

universiteit hasselt | Maastricht University

Transnational University Limburg is a unique collaboration of two universities in two countries: the University of Hasselt and Maastricht University.

universiteit hasselt
KNOWLEDGE IN ACTION

Universiteit Hasselt | Campus Hasselt | Martelarenlaan 42 | BE-3500 Hasselt
Universiteit Hasselt | Campus Diepenbeek | Agoralaan Gebouw D | BE-3590 Diepenbeek

2016•2017
FACULTY OF MEDICINE AND LIFE SCIENCES
Master of Biomedical Sciences

Master's thesis

Investigation of the biological effects of ionizing radiation and iodine deficiency on non-cancerous thyrocytes

Supervisor :
Prof. dr. Niels HELLINGS

Supervisor :
Dr.ir. HANANE DERRADJI

Bertrand Nyuykonge
Thesis presented in fulfillment of the requirements for the degree of Master of Biomedical Sciences

universiteit hasselt | Maastricht University

TABLE OF CONTENTS

LIST OF ABBREVIATIONS

ATC	Anaplastic Thyroid Carcinoma
ATM	Ataxia Telangiectasia Mutated
ATR	Ataxia Telangiectasia RAD3 Related
Bak	Bcl-2 Antagonist/Killer
Bax	Bcl-22 Associated X Protein
Bcl-2	B-Cell Lymphoma 2
Bcl-XL	B-Cell Lymphoma Extra Large
bFGF	Basic Fibroblast Growth Factor
Bq	Becquerel
BRAF-^{V600E}	B-RAF Kinase
cAMP	Cyclic Adenosine Monophosphate
CAT	Catalase
C-cells	Parafollicular cells
CHK1/2	Checkpoint Kinase ½
CK	Casein Kinase
CLIP2	CAP-Gly Domain Containing Linker Protein 2
COX-2	Cyclooxygenase-2
CT	computed tomography
CTNNB1	Catenin β1
DIT	Di-iodinated tyrosine
DSB	Double strand breaks
EMS	Ethyl Methanesulfonate
EFGR	epidermal growth factor receptor
EGF	Epidermal growth factor
ERK	Extracellular-signal regulated kinase
ERR	Estimated relative risk

FNAC	Fine needle aspirate cytology
FOXO3	Fork Head Box O3
FTC	Follicular Thyroid Carcinoma
FRTL-5	Continuous Normal Rat Thyroid Cells
GPX	Glutathione Peroxidase
GSK	Glycogen Synthase Kinase
Gy	Gray
H_2O_2	Hydrogen Peroxide
HIF	Hypoxia Inducible Factor A
HR	Homologous Recombination
HRE	Hormone Response Binding Element
I^{131}	Iodine 131
IAP	Inhibitor Of Apoptosis
ICAM1	Intercellular Adhesion Molecule 1
ID	Iodine Deficiency
IkK	IKβ Kinase
IL	Interleukin
IR	Ionizing Radiation
JAK/STAT	Janus Kinase/Signal Transducer and Activators of Transcription
JNK	JN- Terminal Kinase
LET	Linear Energy Transfer
LNT	Linear No Threshold
MAPK	Mitogen Activated Protein Kinase
Mcl-1	Myeloid Cell Leukemia
MEN2	Multiple Endocrine Neoplasia Type
MIT	Mono-Iodinated Tyrosine
MMPS	Matrix Metalloproteinases
MTC	Medullary Thyroid Carcinoma
mTOR	Mechanistic Target Of Rapamycin

NAI	Sodium Iodide
NF-κβ	Nuclear Factor Kappa Beta
NHEJ	Non-Homologous End-Joining
NIS	Sodium Iodide Symporter
NRF2	Nuclear Factor, Erythroid 2 Like 2
NTRK	Neurotrophin Receptor Kinase
OSI	Oxidative Stress Index
PARP1	Poly [ADP-ribose] Polymerase 1
PAX8/PPARG	Paired Box 8/ Peroxisome Proliferator Activator Receptor Γ
PCCL3	Continous Rat Thyroid Cell Line
PDRX	Peroxyredoxin
PI3K	Phosphatidylinositide 3-Kinases
PKB	Phosphatidylinositol Protein Kinase B
PTC	Papillary Thyroid Carcinoma
PTEN	Phosphatase And Tensin Homolog
ROS	Reactive Oxygen Species
Ser473	Serine 473
SMR	Spontaneous Mutation Rates
SOD	Superoxide Dismutase
SSA	Single Strand Annealing
SSB	Single Strand Break
Sv	Sievert
T3	3,5',3 triiodothyronine
T4	Thyroxine
TBHP	tert-Butyl hydroperoxide
TERT	Telomerase Reverse Transcriptase
TGFβ1	Transforming Growth Factor B1
Thr308	Threonine 308
TNF	Tumor Necrosis Factor

TOS	Total Oxidant Status
TRH	Thyrotropin-Releasing Hormone
TSH	Thyroid Stimulating Hormone
uPA	Urokinase-Type Plasminogen Activator
UV	Ultraviolet
VEGF	Vascular Endothelial Growth Factor
γ-H2AX	Gamma Histone 2A Histone Family, member X

ACKNOWLEDGEMENTS

At the end of my 8 months period at SCK.CEN, I would like to express my gratitude to the friendly and welcoming environment without which this thesis would never have been materialized.

My immense thanks to my SCK.CEN supervisor Dr. Hanane Derradji for her guidance, encouragement, dedication and critical analysis throughout the research work. I equally express my gratitude to Prof. Sarah Baatout for accepting me in her research group, Radiobiology, and for her usual inquiries and encouragement. I would like to thank Prof. Niels Hellings and Jerome Hendriks for their follow-up, support, encouragement and major feedbacks.

I will equally like to express my gratitude to the technicians at Vlaamse Instelling Voor Technologisch Onderzoek (VITO) for their assistance with the comet assay.

I will also like to express my gratitude to my family members for their calls and encouragement especially to Gabrielle and Laura.

I would like to offer special thanks to all the PhD, Master students and technicians at SCK.CEN, Bjorn Baselot, Claude Andre, Noami Daems and Raghda Ramadan and Jasmine Buset and Arlette Michaux respectively for their advice and inputs.

Finally, special thanks to the Almighty God for His guidance and abundant grace throughout the entired project.

SUMMARY

Introduction: The incidence of thyroid cancer is currently on the rise. This could be attributed to advances in screening technologies that enables the detection of small tumors, increased exposure to Ionizing Radiation (IR) and Iodine Deficiency (ID). IR and ID are two risk factors of thyroid cancer that can influence the development of thyroid cancer as seen in epidemiological studies after the Chernobyl nuclear accident. However, the molecular mechanisms from combined IR and ID are unknown and hence the need for our study. We therefore, hypothesized that low dose IR and ID have an additive negative effect on thyrocytes via induction of damaging levels of oxidative stress, potentially leading to activation of precancerous pathways.

Materials and Methods: PCCL3 cells were cultured with or without iodine and X-irradiated with low dose (0 Gy, 0.05 Gy, 0.1 Gy), intermediate dose (0.5 Gy) and high dose (3 Gy) of radiation. Gene expression levels of oxidative stress markers, cell signaling, antioxidant, radiation responsive elements and DNA repair were evaluated by RT-qPCR and western blot. The IncuCyte™ live cell imaging was used to evaluate cell proliferation and apoptosis in real time for 72 hours. Furthermore, a comet assay was used to analyze DNA damage. Finally, ROS production was assessed by CM-H2DCFDA probe. Statistical significance of difference ($p < 0.05$) was evaluated with the TWO-ANOVA test. This was followed by a Bonferroni posthoc test.

Results: IR and ID induced significant cell proliferation in a time and dose-dependent manner relative to the respective iodine sufficient conditions as from 40 hours. For apoptosis, 48 hours after co-treatment we observed cell death at 0.5 Gy and 3 Gy compared to the controls in both iodine conditions. At 72 hours we observed significant cell death at all doses including low doses irrespective of the iodine status. We equally, observed significant changes in anti-apoptotic gene expression (Bcl-2 and Mcl-1) after 24hours. IR and ID equally activated survival and proliferation signaling pathways, JAK/STAT and PI3K/AKT as well as cell cycle regulator Cyclin D2. Furthermore, co-treatment equally induced oxidative stress in a dose-dependent manner which was significant at 0.5 Gy and 3 Gy though we observed no additive effect. However, IR and ID failed to induce DNA damage at all doses at both conditions. Furthermore, antioxidant NQO1 and PRDX5 were equally significantly expressed an indication of ROS burden and antioxidant capacity. Finally, RAD50, a DNA repair molecule was activated by co-treatment at 3 Gy deprived of iodine.

Conclusion: This data indicates that PCCL3 cells are resistance to ID and IR, especially at low doses as we observed cell death mostly at intermediate and high doses at 48 and 72 hours. Furthermore, we observed no significant DNA damage at all doses. Apparently, the cell death observed is not enough to stop cell division as we observed enhanced cell proliferation with iodine deficient conditions. The resistance observed led to activation of mechanisms of proliferation and survival especially PI3K/AKT. Activation of DNA repair signaling molecule and antioxidant molecules observed may also be responsible for the resistance observed against IR and ID. Based on these data, we can conclude PCCL3 cells are highly resistant to the double stress of IR and ID at low doses.

1 INTRODUCTION

1.1 BIOLOGY OF THE THYROID GLAND

The thyroid gland is a ductless, butterfly organ, with a weight of about 25g and is the largest endocrine gland in the body. It is situated in the front of the neck and is made up of the left and right lobes connected by the isthmus. The primary functional unit of the thyroid gland is the follicle, with a rich capillary network and a core of thyroid hormone precursors, (thyroglobulin). The follicle is surrounded by columnal or cuboidal follicular cells, secreting thyroid hormones upon stimulation by Thyroid Stimulating Hormone, (TSH). Within the follicular cells are parafollicular, (C) cells involved in the secretion of calcitonin which controls calcium metabolism. The thyroid gland synthesizes and stores thyroid hormones 3,5',3 triiodothyronine (T3), thyroxine (T4) and calcitonin. These hormones control metabolic activities, body temperature and cardiovascular activities. The synthesis of thyroid hormones is under the control of the hypothalamic-pituitary-thyroid axis. The hypothalamus releases Thyrotropin-releasing hormone (TRH), which stimulates the pituitary gland to release TSH. TSH stimulates the proliferation of the thyroid gland and synthesis of T3 and T4. Firstly, there is the synthesis of thyroglobulin and uptake of iodide via the sodium iodide symporter, (NIS), and oxidation of iodide in the presence of hydrogen peroxide (H_2O_2). This is followed by iodination of tyrosine, the coupling of mono-iodinated tyrosine (MIT) and di-iodinated tyrosine (DIT). Finally, the thyroid hormones are released into the circulation (**Figure 1**). The free T3 binds its affinity receptors in the membranes of target cells and relocates to the nucleus to enhance transcription of target genes. This leads to stimulation of basal metabolic rate, gene expression regulation, differentiation and normal maturation and metabolism of all tissues. (1-3).

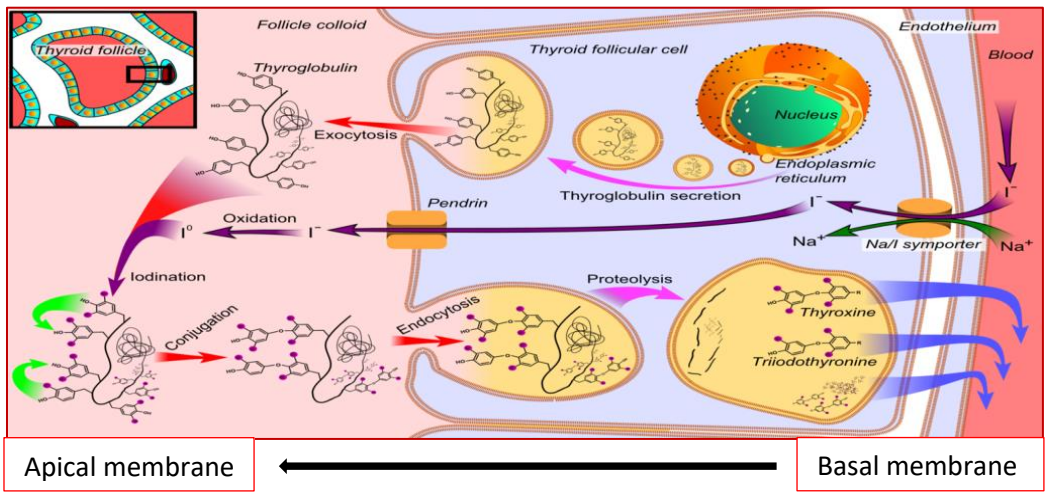

Figure 1: Diagrammatic illustration of thyroid hormone synthesis. First iodide trapping at the basal membrane via the NIS, synthesis of thyroglobulin, organification of tyrosine and coupling. This is followed by the release of thyroid hormones into the circulation. Adapted from Haggstrom *et al.,* 2014.

1.2 THYROID CANCER

Thyroid cancer is the most commonly diagnosed endocrine malignancy. It is responsible for approximately 2% of all newly diagnosed cancers globally. The incidence of thyroid cancer has been on the rise in the past decades globally and continues to rise (4). Incidence varies geographically due to different ethnic and environmental variations including iodine deficiency and radiation exposure. In Belgium, the incidence is equally on the rise, though higher in the Wallonia than Flanders, 6.7 and 3.3 per 100,000 persons per annum respectively. Differences in incidence between the two regions are probably due to more screenings in the south relative to the north (5). The reason for the global rise in incidence is unknown, could be attributed to population exposure to ionizing radiation (IR) from medical and industrial applications and iodine deficiency (ID). This increasing incidence could equally be associated with better diagnosis through advanced technologies such as Fine Needle Aspirate Cytology (FNAC), ultrasound, Computed Tomography (CT) scan and surgery. These technologies enable the detection of tumors with lower diameters (as low as 1mm) not previously detected before. Incidence is three-fold higher in females than males and is age-dependent though molecular factors responsible are poorly understood (6) (7). The differences between male and female incidence are unknown and could be due to hormonal differences. This is because estrogen has been shown to promote thyrocyte proliferation in vitro (8). Though the role of estrogen is not exactly clear since there is no clear demonstrable relationship between thyroid cancer, pregnancy and sex hormone therapy (9). The risk factors associated with thyroid cancer include gender, age, genetic background, IR and ID. There are two types of thyroid cancer, differentiated and non-differentiated (3). Differentiated thyroid cancer is consist of Papillary Thyroid Carcinoma (PTC) and Follicular Thyroid Carcinoma (FTC). Undifferentiated thyroid cancers include Medullary Thyroid Carcinoma (MTC) and Anaplastic Thyroid Carcinoma, (ATC). PTC, FTC and ATC arise from the follicular cells while MTC arises from C-cells of the thyroid gland. Differentiated forms of thyroid cancer are easy to treat unlike non-differentiated, which is aggressive and easily metastasized to other organs like the lymph nodes (4, 10).

PTC accounts for about 80% of all thyroid cancers and common genetic modifications associated with are point mutations, gene translocations and DNA polymorphisms. BRAF-^{V600E} mutation (activating the MAPK pathway), represents about 90% of all BRAF mutations and occur in 45% of sporadic PTC and is specific to PTC. This mutation is associated with poor clinical outcomes, abnormal proliferation, adhesion, migration and invasion and consequently metastasis (11). RAS mutations activate PI3K-AKT pathway, vital in the thyroid cancer tumorigenesis and are associated with 20% of all PTC. RET/PTC translocations are associated with 80% of radiation-induced PTC and 40% of all PTC. RET/PTC1 and RET/PTC3 have been shown to be prevalent in survivors of Chernobyl nuclear accident. Hence an indication that RET/PTC translocations are associated with radiation-induced thyroid cancers. Another chromosomal translocation is the Paired Box 8 (PAX8)/Peroxisome Proliferator Activator Receptor γ (PPARG) present in approximately in 30% of PTC. This PAX8/PPARG complex is a negative inhibitor of PTEN and mutations are associated with thyroid cancer. Other mutations associated with PTC are Telomerase Reverse Transcriptase (TERT), Cyclooxygenase-2 (COX-2), and

Epidermal Growth Factor Receptors (EGFRs) (10). Furthermore, Neurotrophin Receptor Kinase (NTRK), a chromosomal rearrangement is associated with approximately 13% of PTC. (12, 13).

FTC originates from follicular cells of the thyroid gland and accounts for approximately 10% of all thyroid cancers. It has a poor prognosis compared to PTC, 80% of FTC metastasized, hence associated with a higher mortality. More than 50% of FTC are associated with RAS mutations suggesting this mutation is responsible for tumorigenesis. This is because it activates PI3K-AKT pathway involved in proliferation. Common mutations of the PI3K/AKT pathway associated with FTC include PIK3CB, AKT1 and AKT2. PTEN gene, a negative inhibitor of PI3K pathway mutation leading to genomic instability, cancer cell proliferation and survival. This mutation, usually a deletion or silencing, is present in 40% of FTC. Furthermore, PAX8/PPARG complex chromosomal rearrangement is associated with FTC and is prevalent in approximately 60% of FTC. FTC is usually higher in iodine-deficient areas (14, 15).

ATC accounts for approximately 5% of thyroid cancers and is responsible for 40% of thyroid cancer deaths. It emerges from dedifferentiation of differentiated tumors and is resistance to therapy. Silencing of PTEN, a tumor suppressor, by hypermethylation is found in several cases of ATC. Catenin β1 (CTNNB1) vital in WNT-β-catenin pathway is mutated in ATC by upregulation of c-myc and Cyclin D1. Tumor suppressor p53 (TP53) mutation is associated with 70-80% of ATC and is responsible for genomic instability, uncontrolled proliferation. This is due to downregulation of pro-apoptotic proteins like Bax and FAS and upregulation of Bcl. RAS mutations are detected in 25% of all ATC cases. Mutations in TERT have been described in up to 50% of ATCs especially in association with BRAF and RAS mutations (14, 16).

MTC is calcitonin-producing tumor that accounts for approximately 5% of all thyroid carcinomas and arises from C cells of the thyroid gland. Eighty percent of MTC occur as sporadic while familial MTC accounts for 20% which is autosomal dominant. This familial MTC is associated with RET mutations. There are three types which include multiple endocrine neoplasia type 2A, (MEN2A), multiple endocrine neoplasia type 2B (MEN2B) and familial medullary thyroid carcinoma (FMTC). RAS mutations have been detected in about 40% of sporadic MTCs (17, 18).

Despite the advances made to understand the molecular mechanisms of thyroid cancer the incidence is still on the rise. It has been suggested that environmental or modifiable risk factors like ID and IR could be responsible. This is probably because two billion people still suffer from ID globally and the population is increasing being exposed to low-dose IR from medical and industrial applications. Therefore, it is vital to investigate the cellular and molecular effects of these two stressors in non-cancerous thyrocytes. This will help to establish the mechanisms by which these two important factors may influence the development of thyroid cancer.

1.3 RISK FACTORS OF THYROID CANCER

1.3.1 IONIZING RADIATION

1.3.1.1 Biological effects of ionizing radiation

Ionizing radiation possesses much energy capable of freeing electrons from molecules making them ionized. The different forms of ionizing radiation are low linear energy transfer (LET), such as x-ray, γ-rays and higher ultraviolet part of the electromagnetic spectrum (High LET). The "absorbed" dose refers to radiation dose absorbed by a specific organ or tissue per unit mass and is measured in Gray (Gy). The Sievert (Sv) is the unit of measurement of ionizing radiation dose and measures the "effective" dose which assesses long-term effects from non-uniform exposure. The Becquerel (Bq) measures the amount of activity which results from radioactive substances (19, 20). The major sources of background radiation are cosmic, external terrestrial, radon and thoron from internal exposure. Man-made sources of radiation result from industrial, diagnostic and therapeutic applications such as X-ray, CT scans and radiotherapy. The average exposure from the background and human-made radiation in Belgium stand at 4.5mSv higher than the global exposure, 3.7mSv. The high average exposure has led to a double in average effective dose in Belgium in the last century from 2.3mSv to 4.5mSv (1900-2001). Though the majority of this increased exposure in Belgium could largely be attributed to medical applications especially CT scan (**Figure 2A**) (21). Radiation exposure has two biological effects, which are deterministic and stochastic effects. Deterministic effects refer to the acute harm on tissues due to killing and malfunction of cells such as skin reddening and burns after high dose exposure (2.5-6Gy). Stochastic effects refer to cancer and heritable effects due to mutations following exposure to low dose IR with no specific threshold. The Linear Non-Threshold model (LNT) is used to quantify radiation exposure and regulate limits. The LNT hypothesized that long-term biological damage from low dose radiation is directly proportional to absorbed dose with no consideration to dose rate. However, there is no evidence or data to prove low doses less than 100mSv is carcinogenic (**Supplementary figure 1**). According to the Hormesis model, low dose radiation has beneficial health effects referred to as hormesis effect. However, Hormesis model remains very controversial as well due to lack of justifiable data. The Threshold model simply implies that below the 100mSv there is no risk while the Hypersensitivity model suggests there is a greater risk below the 100mSv threshold (22). The biological effects of radiation depend on the time of exposure, distance to the source and shielding. Ionizing radiation especially high-LET interact with vital tissue organization hence capable of much destruction upon internal contamination. Low LET IR gives rise to Reactive Oxygen Species (ROS) through interaction with intracellular water molecules since it is highly penetrative and hence responsible for the long-term biological effects. The biological effects could be direct irradiation of cells or through bystander effects on neighboring cells. IR leads to DNA damage directly or indirectly such as double-strand breaks (DSBs), genetic instability, mutagenesis and inflammatory response. There is activation of TP53, Ataxia Telangiectasia Mutated (ATM) and Ataxia Telangiectasia RAD3 Related (ATR) in response. Failure consequently could result in genomic instability through poor DNA Damage Response (DDR) and radiation-induced apoptosis and aging. This leads to further activation of survival and proliferation pathways such PI3K/AKT and MAPK signaling pathways. This consequently could lead to increase mutations, translocations and other effects to enhance precancerous transformations (23) (24).

1.3.1.2 Risk of thyroid cancer following exposure to ionizing radiation

IR exposure, especially in children is an established risk factor associated with the development of thyroid cancer. This follows epidemiological studies in the former USSR countries (Russia, Ukraine and Belarus) exposed to higher doses of radiation doses following the Chernobyl nuclear disaster. The incidence of thyroid cancer was found to be approximately a 100 fold higher in some areas exposed to radiation from the Chernobyl nuclear plant (25, 26). This was particularly higher in the population who were either children or adolescent at the time of exposure. Children were more vulnerable as they possessed a proliferating and radiosensitive thyroid gland susceptible to DNA damage. One of the main components of this IR was radioactive iodine (I^{131} 1,760PBq) which is highly taken up by the thyroid and led to internal contamination. Furthermore, the incidence and the Estimated Relative Risk (ERR) was much higher in females than males (27-29). In another study to determine the long-term effects of the Nevada bomb and Marshal Islands tests, a suggested increased risk of thyroid cancer from nuclear fall outs was observed (30). Additionally, a study after the Fukushima earthquake nuclear plant accident to screen for thyroid malignancy was conducted over half a decade. There was an overall increased in the incidence of thyroid cancer though it was too early to relate the increased incidence to radiation exposure. The researchers suggested the increase in incidence had resulted from very sophisticated ultrasound techniques that were used for screening (31). Moreover, in a study in French Polynesia to evaluate the effects of Atomic bomb testing on the risk of thyroid cancer, a low risk of thyroid cancer was associated with the test though this was hindered by much of the data being classified (32). In Belgium, (NUCABEL studies), researchers carried out a study to investigate the incidence of thyroid cancer within the population around the various nuclear sites, (Mol-Dessel and Fleurus). They reported there was no excessive incidence but a higher incidence was observed in Mol , where other industries are located hence the results were not conclusive (33). Despite these associations with thyroid cancer, it is not clear how radiation exposure contributes to increasing incidence though the increases are mostly with PTC, which is associated with radiation exposure (34).

Medical applications such as CT scan, X-ray and radiotherapy account for another major source of radiation linked to thyroid cancer globally and in Belgium (**Figure 2B**). One-third of CT scans are performed on the head and neck, which exposed the thyroid gland to radiation. The use of radioactive material applications in the head and neck leads to increased "absorbed" doses by the thyroid. The risk assessments from medical exposure are mostly based on statistical models from atomic bomb survivors. Hence, there is equally a need to confirm this by epidemiological studies (35, 36). In a study to assess the risk associated with radiotherapy in patients with tinea capitis in Israel, a significant risk was associated with thyroid cancer (37) Furthermore, a study evaluating external beam radiation to treat Hodgkin's lymphoma, benign diseases like tonsillitis, acne and adenitis showed an increase in thyroid cancer risk of up to 9 fold per Gray (38, 39).On the contrary, there was no substantial risk related to the development of thyroid cancer due to exposure from X-rays in a similar study in Sweden (40, 41). Furthermore, a study evaluating the risk of thyroid cancer from use of ^{131}I in radiotherapy in adults showed no significant risk associated with thyroid cancer. It was suggested that internal exposure did not occur early in life when the thyroid is vulnerable to radiation (42). In another study, investigating X-ray exposure to the skull, head, neck, chest, teeth and breast. The researchers found no significant risk associated with these procedures but for dental X-ray which was associated with increased thyroid cancer risk.

A

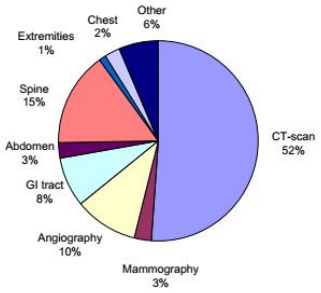

B

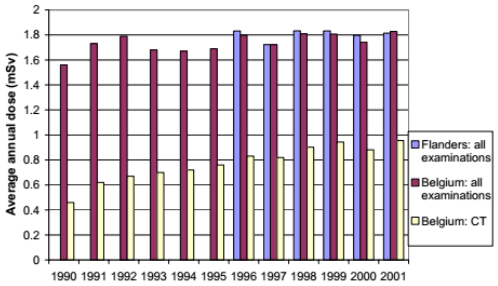

Figure 2: Belgian population exposure to Diagnostic Radiation. **A**) Dose distribution from diagnostic radiology in the Flemish region in 2001. CT scan accounts for than 50% compensated by a decrease in conventional sine, lumbar and GIT examinations. **B)** Trends in annual effective dose in Belgium and Flanders (1999-2001) from diagnostic radiation. The average effective dose in Flanders and Belgium is approximately 2mSv in 2001. *Vanmarcke et al., (18)*

1.3.2 IODINE DEFICIENCY

Iodine is a rare element that is needed in the synthesis and metabolism of the thyroid hormones thyroxine T4, T3 and calcitonin. Iodine deficiency is associated with, mental and physical retardation, miscarriages, endemic goiter and other malignancies. In addition to low dietary intake, other factors related to iodine deficiency include selenium deficiency, pregnancy, gender, radiation exposure and iodine antagonists like bromine and perchlorates (43). There is a strong correlation between goiter and thyroid carcinogenesis and iodine deficiency as clinically relevant thyroid nodules are frequent in iodine deficient areas. This is as a higher thyroid cancer incidence has been observed in Switzerland, in areas which were previously goiter endemic. A study in the female population of New Caledonia, with a high incidence of thyroid cancer, investigated the role of cruciferous vegetables and seafood on the incidence of thyroid cancer for a 5year period. The results showed there was a high association between thyroid cancer incidence and consumption of cruciferous vegetables compared to the population that consumed seafood rich in iodine (4, 44). In another study in French Polynesia, which equally has a high incidence of thyroid cancer and iodine deficient. An approximate threefold increase was associated with iodine deficient subjects compared to iodine sufficient population (45). Furthermore, a similar study in Tasmania following the withdrawal of iodine supplementation (potassium iodide) prophylaxis showed an increase in thyroid cancer incidence. On the contrary, reports from Hawaii, Japan and Iceland contradicts this reports as they have a higher incidence of thyroid cancer (especially PTC) despite being iodine sufficient. The increased incidence in Iceland could be attributed to the volcanic nature of the island resulting in increased natural radiation exposure. Also, South Korea has one of the highest incidence of thyroid cancer even though not iodine deficient. It is suggested that the observed higher incidence in South Korea correlated with excessive iodine intake which is associated with BRAF mutations (46). Despite these studies, there is no clear relationship between population iodine status and thyroid cancer incidence.

Possible mechanisms by which ID initiates thyroid cell malignancy have been suggested. Iodine deficiency leads to a decrease in the synthesis of thyroid hormones, T3 and T4, followed by an increased in NIS turnover. This results in a subsequent increase in TSH secretion by upregulation of calcium ions and cAMP, both intracellular messengers. This is followed by hyperplasia, characterized

by increased cell proliferation. This limits the ability of thyrocytes to concentrate iodine and subsequently thyroglobulin (47). This increased proliferation is accompanied by increased secretion of Epidermal Growth Factor (EGF), Fibroblast Growth Factor (bFGF). Increased TSH secretion equally leads downregulation of Transforming Growth Factor β1 (TGFβ1). TGFβ1 is vital in thyroid growth and cell inhibition hence ID may result in high proliferation by down-regulation TGFβ1. ID equally leads to vascular changes in the thyroid gland by a TSH-independent reactive oxygen species (ROS)-hypoxia inducible factor (HIF)-αVEGF pathway (48, 49). Studies have shown increased serum levels of Vascular Endothelial Growth Factor (VEGF) in thyroid cancer patients suggesting its role in pathogenesis. ID stress induces ROS production by phosphorylation of pSer1177. Iodine equally acts as an antioxidant hence a deficiency permits the accumulation of ROS (50). The oxidative stress leads to DNA and cellular damage and possibly genomic instability by interaction with tissue architecture. In an animal study evaluating the effects of ID, a significant increase in antioxidants such as Superoxide Dismutase 3 (SOD-3) and catalase (CAT) was observed. There was equally upregulation of peroxiredoxins (PDRX) especially 3 and 5 an indication of ROS burden. Furthermore, there was an increase in glutathione-dependent enzymes such as glutathione-s-transferase and glutathione peroxidases 2,3 and 4. This increased expression and activities of these ROS scavengers confirmed the presence of oxidative stress from ID (51) (52).

Apart from the thyroid gland, there are several tissues (extrathyroidal tissues) with the ability to concentrate iodine via expression of NIS and pendrin in their basal and apical membranes respectively. These tissues include but not limited to stomach mucosa, salivary gland, lactating mammary glands, placenta, uterus, prostate and pancreas. This is due to the property of iodine to act as an antioxidant, anti-inflammatory, differentiation and proapoptotic agent. In the lactating mammary glands, iodine is taken up to supply the newborn with the necessary iodine before self-sustenance. Iodine plays its antioxidant role by its ability to act as an electron donor to free radicals or through organification of tyrosine and unsaturated fats limiting their capacity to react with ROS. Furthermore, the anti-inflammatory or antibacterial activity of iodine is through neutralizing ROS and inhibiting production of nitric oxide, prostagladine-E2, IL-6 and TNF-α. Iodine mediates apoptosis by disruption of mitochondrial potential initiating mitochondrion-driven apoptosis or through the formation of iodolipids. Iodine could also trigger apoptosis by activation of PPARγ triggering Bax-caspase pathway. Based on this, ID may act as a risk factor for cancer initiation and progression in the above mentioned extrathyroidal tissues. Hence, ID is associated with stomach, breast, prostate and other types of malignancies (53).

1.3.3 COMBINED EFFECTS OF IONIZING RADIATION AND IODINE DEFICIENCY ON THYROCYTES.

After the Chernobyl accident in 1986, the population around the nuclear power plant was exposed to ionizing radiation especially to radioiodine (^{131}I). This consequently resulted in a higher incidence of thyroid cancer of the PTC histotype particularly in pediatric and adolescent population in exposed areas. This incidence was remarkably higher in iodine deficient areas compared to iodine sufficient areas. The incidence in children was higher than adults because children have a higher proliferating thyroid gland. It has been suggested that the higher incidence in iodine deficient areas was due to

the thyroid gland's high affinity for radioiodine. This is because ID leads to increased blood flow, size and proliferation of the thyroid rendering it susceptible to rapid uptake and concentration of I^{131}. (54, 55). There was a threefold increase in the risk of developing thyroid cancer in iodine deficient areas, but the risk reduced equally by threefold following potassium iodide supplementation. This suggests that iodine supplementation can slow proliferation and therefore, reduced thyroid cancer risk. Based on the above studies, it is possible to reduce the risk and high incidence of thyroid cancer by eliminating ID (28, 56). Failure to eliminate low iodine intake can act together with ionizing radiation to favor a substantial increase in the risk of developing thyroid carcinomas.

Despite these few epidemiological studies on radiation and ID after Chernobyl, there have been only few animal studies on the combined effects of radiation and iodine deficiency. In one of such studies, young mice (4weeks), were fed with varying iodine diets (low, normal and high) and evaluated for 110weeks. The animals were exposed to a single dose of high radiation (4Gy) after 40days. Both excessive and deficient fed animals developed thyroid adenomas before irradiation while sufficient iodine mice did not. Iodine deficient and iodine excessive animals equally developed significant adenocarcinomas (50-80%) following high dose irradiation. The absence of carcinomas in iodine sufficient mice suggested that normal iodine intake could have the ability to reduce or to inhibit radiation-induced thyroid carcinogenesis. Therefore, ID can act as a promoter and a weak carcinogen in the development of thyroid cancer (57, 58). However, there has been no study conducted with regards to the molecular mechanisms of combined ionizing radiation and ID to the best of our knowledge. Therefore, it is necessary to identify the potential mechanisms by which these two factors may act together to initiate thyroid cancer. This is because two billion people still suffer from ID nowadays and there is increase exposure to low dose radiation from medical and industrial applications.

1.3.4 POTENTIAL CELLULAR AND MOLECULAR MECHANISMS INDUCED BY THE COMBINATION OF IONIZING RADIATION AND IODINE DEFICIENCY ON THYROCYTES

1.3.4.1 Oxidative stress

In the thyroid gland, H_2O_2 results from activation of one or two NADPH oxidases (Duox1/2) and is vital in thyroid hormone biosynthesis. Low and moderate levels of endogenous ROS are present in the cells and is needed for defense, cell proliferation, survival and differentiation. The normal levels of ROS are maintained in the cells by antioxidants such as superoxide dismutase (SOD), Catalase (CAT), glutathione peroxidase and peroxiredoxin (PRDX). Chronically increased endogenous ROS generation leads to tumorigenesis and metastasis. DNA damage from radiation-induced ROS results from the direct interaction of ROS with nuclear DNA, oxidation of DNA precursors or inhibition of enzymes vital in nucleotide synthesis. (59). This excessive ROS generation from IR leads to further DNA damage, genome instability, cell aging, apoptosis and necrosis, and transformation. It has also suggested that this ROS-induced DNA damage leads to gene mutations or alterations (BRAF, Ras, PIK3CA, RET/PTC, and PTEN) that could promote malignant transformation. These genetic alterations could activate precancerous pathways such as Mitogen-activated protein kinases (MAPK) and

Phosphoinositide 3-kinase (PI3K) pathways to enhance premalignant proliferation (60, 61). The production of matrix metalloproteinases (MMPs) and inflammatory cytokines such as TNF-α and TGFβ1 have been stimulated by ROS following exposure to cellular stresses like radiation and ID. These MMPs which are stimulated by overexpression of MnSOD and cytokines are involved in BRAF mutations linked with the thyroid cancer development. This H_2O_2 acts as a substrate for thyroperoxidase and thyroglobulin iodination and responsible for DNA damage. Studies by Huang et al., 2008 evaluating Total Oxidant Status (TOS) and Oxidative Stress Index (OSI) in cancer patients showed increased in TOS and OSI in thyroid autoimmune diseases and thyroid cancer. (62, 63). Furthermore, in another study, radiation-induced H_2O_2 led to RET/PTC1 rearrangements in thyrocytes after exposure to 5 Gy of X-ray (64). This suggests ID and radiation could lead to enhance oxidative stress and could therefore act together to release harmful levels of ROS which can lead to pre-malignant transformation. So, we will investigate oxidative stress following co-treatment of cells with ID and ionizing radiation, especially low dose ionizing radiation. We will equally investigate gene expression changes in antioxidant genes such as CAT, PDRX and NQO1 vital in ROS scavenging and indicative of ROS burden.

1.3.4.2 DNA damage response and apoptosis.

Ionizing radiation leads to DNA damage directly by interaction with DNA or indirectly by the generation of ROS. Double Strand Breaks (DSBs) are the most renowned lesions as a single DSB can lead to cell death especially mitochondrial-mediated as mt-DNA is more vulnerable to IR. Following DSB, the cell cycle is stopped to permit repair by the cell's machinery. Sensor proteins such as RADs, NF-κβ, ATM/ATR act directly on the lesion by phosphorylation of effector kinases like Check Point Kinases (CHK1/CHK2), leading to cell cycle arrest and apoptosis. Cell cycle arrest following DNA damage by IR, involves upregulation of p53 and its transcriptional targets such as inhibitory growth genes like p21cip1/waf1 and GADD45. P53 coordinates the repair of damaged DNA, cell cycle progression and apoptosis thereby ensuring genome stability. Failure of the p53 due to mutations (from IR) to repair the damage leads to accumulation and transfer of mutations to daughter cells. Ionizing radiation can equally induce cell death through the mitochondrial apoptotic pathway by suppression of Bcl-2 and induction of Bax transcriptions. IR equally activates the death receptor pathway by up-regulation of death receptors and their ligands as seen in studies of breast cancer cells where FAS was upregulated by UV radiation (23, 65). Thyrocytes have been shown to upregulate glutathione peroxidase (GPX) transcription in response to H_2O_2 and increased DNA damage especially DSBs after irradiation. These DSBs are repaired by either homologous recombination (HR), non-conservative homologous recombination, single strand annealing (SSA) and non-homologous end-joining (NHEJ) pathways. HR is an accurate pathway for the repair of DSB and this is by obtaining the appropriate sequence from a homologous strand of intact DNA. The SSA and NHEJ are much error-prone since there are possible modifications and losses at the end. NHEJ, the DNA strands are cut or modified and ends ligated together irrespective of homology leading to possible deletions and insertions. This is characterized by nuclease-mediated resection of damaged DNA ends, polymerization of new DNA, ligation and restoration of double strand integrity. Some of these damages include pyrimidine and purine lesions which affect genome integrity. 8-oxo-7,8-

dihydroguanine is the most extensively studied product due to its mutagenic nature and ability to be detected immunologically. Therefore, it is often used as a marker of DNA damage resulting from oxidative stress. Signal transduction pathways response to DSBs and SSBs involves ATM and ATR respectively. The Mre11/Rad50/Nbs1 (MRN) complex interacts with ATM at the damage site helping to phosphorylate its substrate as well as ATR signaling. Unlike ATM which is responsible for DSB repair, ATR is responsible for DSBs and other DNA lesions repair. The activation of ATM is vital to activate cell cycle checkpoint arrests (G1/S boundary and prevention of entry into mitosis, G2/m) or apoptosis. Phosphorylation of histone variant, H2AX to γ-H2AX is a common phase in both ATM and ATR signaling and hence γ-H2AX is a common biomarker of double strand breaks (66, 67). Our preliminary studies indicate PCCL3 and FRTL5 are resistant to DNA damage by high dose IR and ID when measured by γ-H2Ax. We will further investigate most of these genes involved in DDR such as ATM, RAD50 and p53 in PCCL3 at different time points and apoptosis. Furthermore, we will investigate chromosome and chromatid damage as a result of co-treatment.

1.3.5 ALTERED SIGNALLING PATHWAYS IN THYROID CANCER

1.3.5.1 The MAPK signaling pathway

The Mitogen-Activated Protein Kinase (MAPK), is an intracellular serine/threonine protein kinase in mammals with diverse signaling pathways. These include Extracellular-signal-Regulated Kinase (ERK), c-JUN-terminal Kinases/Stress-Activated Protein Kinase (JNK/SAPK), p38MAPK, and ERK5/BMK1 (Big Mitogen-Activated Protein Kinase 1). This pathway is vital in cell proliferation, differentiation, senescence and apoptosis (68). Cellular stress such as ID and radiation, especially UV-radiation has been shown to activate JNK to induce programmed cell death and inhibition of JNK by AKT to inhibit apoptosis. ROS production equally leads to secretion of pro-inflammatory cytokines like IL-1β and TNF-α, which leads to activation of p38MAPK. (**Supplementary figure 2**). This pathway is activated by tyrosine receptor kinases and cytokines and then transduce external signals into the nucleus to initiate proliferation, differentiation, apoptosis. Overactivation of this pathway following IR and ID exposure leads to upregulation of proto-oncogenes. These proto-oncogenes include VEGFA, MMPs, prohibitin, vimentin, NK-KB, HIF1α, thromboplastin 1, prokineticin and TGFβ. These oncoproteins enhanced cancer cell proliferation, migration and growth, survival, angiogenesis, invasion and metastasis. This over-activation has also been strongly associated with mutations like $BRAF^{v600E}$ which is linked to thyroid cancer (69). Furthermore, RAS and RET/PTC, known mutations in thyroid cancer have been proven to activate MAPK pathway. TGFβ1 activation results in an inflammatory microenvironment leading to the production of high levels of ROS, which further over stimulate the MAPK pathway. General alterations in MAPK pathway are often associated with PTC. Hence, these MAPK pathways can determine cell fate following exposure to IR and ID exposure (70).

1.3.5.2 PI3K/AKT signaling pathway

PI3K is an intracellular signal transducer (downstream of EGFR) that catalyzes the phosphorylation of Phosphatidylinositol protein Kinase B (PKB) or AKT. PI3K/AKT signaling regulates cell survival and proliferation, DNA repair, cell cycle progression, differentiation, angiogenesis, glucose and protein

synthesis and cell migration. Phosphorylated PKB, (p-AKT) is an activated form of AKT by phosphorylation at Thr308 and Ser473 capable of activating biological changes that could inhibit by PTEN. ROS especially H_2O_2 following exposure to IR or ID, activates this pathway by increased phosphorylation at Thr308 and Ser473. The activated p-AKT subsequently activate downstream elements such as caspase 9, Bad, fork-head, Par-4, p21 and mechanistic target of rapamycin (mTOR). The phosphorylation of forkhead directly inhibits apoptosis by inhibiting transcription of FASL. p-AKT is also capable of inhibiting activation of proapoptotic caspases like 3, 7 and 9 by phosphorylation of Inhibitors of Apoptosis (XIAP). PI3K/Akt/mTOR induced tumorigenesis by preventing autophagy activating VEGF/HIFα pathway. This leads to angiogenesis associated with the early phase of tumorigenesis. (71, 72). Activation of PI3K/AKT signaling pathway further leads to activation of other pathways such as forkhead box O3 (FOXO3), Wnt-β-catenin and NF-κβ pathways which are vital to survival (73). Activated PI3K/AKT also inactivate Bax Bad by phosphorylation of Ser184 to inhibit apoptosis. Activating mutations associated with this pathway are RAS, RTK, peroxisome proliferators-activated receptor γ/paired box gene 8 (PPARγ/PAχ8) and PTEN. PTC due to MAPK activation could be dedifferentiated to FTC and further to ATC by activation of the PI3K pathway. Furthermore, AKT activation also lead to translocation of NF-KB to the nucleus and transcription of its regulated genes like Bcl-xl, Bcl-2 which promotes proliferation and survival by inhibiting apoptosis. It equally activates mTOR kinase, which phosphorylates induced myeloid leukemia cell differentiation protein (Mcl-1), an anti-apoptotic protein (**Supplementary figure 3**). The activation of this pathway by ROS equally leads to genetic instability. This is by probably through destabilization of the tumor suppressor P53, enabling survival of cells with damage DNA to escape apoptosis t(74). So, the activation of this pathway will be investigated following co-treatment with IR and ID.

1.3.5.3 NF- κβ signaling pathway

The Nuclear Factor Kappa β (NF-κβ) proteins are heterodimers with five members including Rel (cRel), p65 (RelA, NF-κβ3), RelB, p50 (NF- κβ1), p52 (NF- κβ2) and Iκβ (Inhibitor of Kappa β) (**Supplementary figure 4**). Iκβ consists of IKKγ, IKKδ, IKKε and Bcl-2, which act to inhibit the activity of NF-κβ and is known to be activated upon exposure to UV-radiation. This pathway is vital in regulation of stress response, apoptosis and inflammation associated with thyroid tumorigenesis following exposure to radiation. ROS production induced by IR is vital in NF-κB signaling through the regulation of cytokines such as TNF-α, IL-1β and IL-6. It also enables the upregulation of anti-apoptotic gene expressions such as Bcl-2 and cellular inhibitor of apoptosis proteins (c-IAP1 and c-IAP2). DSBs which result from irradiation leads to ATM for NF-κB activation independent of TNF-α. Apart from the latter, TNF-β, IL-6, IL-1, ICAM1, cyclin B1 and cyclin D1 are other targeted genes by radiation-induced activation of NF-Kβ. These effector genes could equally play a vital role in tumor initiation and promotion by inhibiting apoptosis and promoting survival and proliferation of mutated cells. Regulation of NF-κβ in thyroid cancer cell lines enhanced cell proliferation and inhibiting apoptosis. Ionizing radiation activates this pathway which enables cell cycle arrest and inhibition of apoptosis enabling cells to optimize DNA repair or resist apoptosis. This continuous suppression of apoptosis by NF-Kβ enable cells to accumulate mutations to enhance their survival or resistance to

radiation-induced damage and hence continue to proliferate. Ionizing radiation equally activates this pathway independent of DNA damage by activation of P38MAPK pathway degrading IκB-β through activation of casein kinases (CK 1 and CK2) (75, 76). NF-Kβ activation in thyroid cancer is associated with PTC, FTC and ATC and promotes dedifferentiation of PTC and FTC. NF- κβ pathway activation is associated with progression and invasiveness by upregulating expression of MMPs, IL-8 and urokinase-type plasminogen activator (uPA) (77). We will also investigate the activation of this pathway following co-treatment with IR and ID.

1.3.5.4 JAK/STAT signaling pathway

The Janus Kinase/Signal Transducer and Activators of Transcription (JAK/STAT) pathway is a vital signaling pathway activated by cytokines, growth factors possibly oxidative stress (**Supplementary figure 5**). It is vital in the stimulation of cell proliferation, differentiation, migration and programmed cell death. Dysregulation of this pathway is associated with tumorigenesis through unregulated proliferation and inhibition of apoptosis. For instance, STAT3 is constitutively active in 95% of head and neck cancers including thyroid cancer and is responsible for the malignant behavior of cells (78). There is evidence of the JAK-STAT activation following IR by the generation of ROS. This is by the mediation of ATM, Chk1, CHK2, ATR and H2AX vital in phosphorylation of key molecules involved in repair and apoptosis. Activated STAT3 increased Bcl-2, Bcl-xl and other surviving genes like cyclin D1 (CCND1), CCND2 and c-myc hindering caspase 3 activity and hence apoptosis. This activation could equally regulate expression of VEGF, MMP-2 and collaborate in tumorigenesis by cross-talking with HIF1α and NF-κβ. Moreover, activated STAT3 by RET/PTC induced Tyr705 phosphorylation leads to upregulation of VEGF, CCND1, CCND2 and intercellular adhesion molecule 1 (ICAM1) (79). STAT3 knock-down by mediated shRNA lead to the generation of larger thyroid tumors and facilitated tumorigenesis in B-Raf^{V600E} induced PTC (80). Hence, we shall evaluate the expression of STAT3 as an indication of activation of the JAK/STAT pathway which could be dysregulated following co-treatment.

1.4 RESEARCH PLAN

The main aim of this project was to evaluate cellular and molecular changes in thyrocytes following treatment with IR, especially low dose and ID. We focused on PCCL3 cells because our research group had investigated the effects of this double treatment on FRTL5 and also did some preliminary work on PCCL3. It is known from the literature and our preliminary results that IR and ID can lead to the cellular stress leading to the production of ROS (oxidative stress). Based on this, we therefore, hypothesized that low dose IR and ID have an additive negative effect on thyrocytes via induction of oxidative stress, potentially leading to activation of precancerous pathways. To achieve our aim, normal rat PCCL3 cell lines were cultured in the presence or absence of sodium iodide (10^{-8}M NAI) at physiological concentration. This was to mimic iodine deficient and sufficient conditions. In each iodine status, cells were X-irradiated with 0.05 Gy and 0.1 Gy (low dose), 0.5 Gy (intermediate dose) and 3Gy (high dose). In addition to these conditions, we had a control in which the cells were sham-irradiated. This was followed by further investigation of oxidative stress by measuring

expression levels of oxidative stress biomarker, Nuclear Factor Erythroid 2-related Factor 2 (NRF2). Measurement of ROS production following co-treatment was evaluated with CM-H2DFCDA probe. DNA damage due to the co-treatment was quantified by the use of the comet assay and intensity of comet quantify by fluorescence microscopy. This was followed by evaluation of gene expression changes involved in proliferation, survival, antioxidant defense, radiation responsive element and DNA repair by RT-QPCR. Finally, Cell proliferation was evaluated by the IncuCyte™ Zoom proliferation assay and apoptosis, Caspase-3/7 and Annexin V multiplex kinetic assay were performed with the IncuCyte™ Zoom to determine the proportion of living, early apoptotic, late apoptotic and necrotic cells (**Supplementary figure 6**).

2 MATERIALS AND METHODS

2.1 CELL CULTURE AND IRRADIATION

PCCL3, a clonal rat thyroid cell line requiring TSH for growth, were grown to attain 80-90% confluence for 7 days in Coon's modified Ham's F12 supplemented with the following 5% fetal bovine serum (FBS) (Gibco, Ghent, Belgium), 2.4 mM glutamine (Sigma-Aldrich, Diegem, Belgium), 1mU/mL TSH (Sigma-Aldrich, Diegem, Belgium),100 u/mL penicillin-streptomycin (Invitrogen, Ninove, Belgium), 2.5 µg/mL Fungizone (Invitrogen, Ninove, Belgium), 1 µg/mL insulin (Sigma-Aldrich, Diegem, Belgium) and 5 µg/mL transferrin (Sigma-Aldrich, Diegem, Belgium) containing physiological NAI of 10^{-8} M in a humidified atmosphere (5% CO_2 and 37°C). On the day of the experiments, the cells were washed with phosphate-buffered saline (1x PBS) (Gibco, Ghent, Belgium) and culture media were replaced with fresh media with, (control) or without NAI. This was followed by X-irradiation of cells with low (0.05 Gy and 0.1 Gy), intermediate (0.5 Gy) and high (3 Gy) radiation doses at the rate of 0.124 Gy/minute using the Xstrahl 320 kV generator. The control cells which were not exposed to ID received a sham irradiation. Samples were later harvested according to the experimental timelines (6, 24 and 72 hours).

2.2 RNA ISOLATION AND REVERSE TRANSCRIPTION

Three days to co-treatment with ID and IR, cells were transferred into six 6-well plates (3 x 10^5 cells/well) for cell analysis after co-treatment with ID and IR. Each of the five 6-well plates represented a single radiation dose mentioned above, with three biological and technical replicates of iodine sufficient and deficient conditions. The cells were washed twice with 1x PBS and lysed in 350 µl of RNeasy Lysis Buffer Plus from Qiagen RNeasy Plus Mini Kit (Qiagen, Antwerp, Belgium). Whole RNA was purified according to manufacturer's instructions and resuspended in 40 µl of nuclease-free water. The quantity and purity of the RNA was evaluated respectively using the DropSense 16 spectrometer (Trinean, Ghentbrugge, Belgium) and RNA Integrity Number (RIN) (Agilent's lab-on-chip Bioanalyzer 2100, Agilent Technologies Diegem, Belgium). This was followed by 2 µg of total extracted RNA being reverse transcribed to cDNA with the GoScript Reverse Transcription System (Promega, Leiden, Netherlands) according to the manufacturer's instructions. Briefly, 2 µg of total RNA was mixed with 1 µg of random primers and 1 µg of oligo $(dT)_{15}$ primers an appropriate volume of nuclease-free water, thermally denatured at 70° C for 5minutes. This was followed by 8 µg GoScript 5x reaction buffer, 6 µl $MgCl_2$, 2 µl PCR nucleotide mix (0.5 mM of each dNTP), 1 µl recombinant RNasin ribonuclease inhibitor and 2 µl GoScript reverse transcriptase were added. The final solution was incubated for 5minutes at 25 ℃ to permit primer annealing, at 42 ℃ for 60 minutes to allow the first strand synthesis of cDNA and then 70°C for 15minutes to inactivate reverse transcriptase. The obtained cDNA samples were stored at -20 C for further analysis.

2.3 GENE EXPRESSION BY REAL TIME PCR

Following cDNA synthesis, RT-qPCR was performed using the TaqMan® Gene Expression Assays (Thermo Fisher-Invitrogen-Life Technologies Gent, Belgium). The qPCR 20 µl reaction mixture included 10 µl TaqMan advance master mix, 2 µl of cDNA template, 1 µl of selected primers (forward and reverse primers) (TP53, NQO1, VEGFA, ATM, RAD50, CAT and PRDX5, Bcl-2, Mcl-1, AKT1, and STAT3) and 7 µl of nuclease free water. The reaction mixtures were centrifuged for 1 minute to eliminate air bubbles. Finally, the mixtures were incubated for an initial activation at 95°C for 5 minutes and 30 seconds, followed by 40 cycles of 95°C for 15 seconds, annealing temperature for 45 seconds, and 81°C for 30 seconds using ABI 7500 Fast system (Applied Biosystems). Experiments were performed in triplicates and levels were normalized against those of β-actin.

2.4 WESTERN BLOT FOR PROTEIN DETECTION

Two million cells/flask were seeded in 75-cm^2 cell culture flasks in medium with iodine for five days and then transferred to five six well plates for three days. Each experimental condition had three biological replicates. On the day of the experiment, the medium in each well was refreshed with new medium either containing or not iodine depending on the experimental condition. One hour after irradiation, the cells were harvested by trypsinization (0.05% Trypsin-EDTA) and the cell pellets kept at -80°C till protein extractions. Proteins were isolated from the cells using the Bio-Rad's ReadyPrep II including 8 M urea, 4% CHAPS, 40 mM Tris and 0.2% Bio-Lyte 3/10 ampholyte (Bio-Rad, Temse, Belgium) supplemented with 0.5 Complete Mini Protease Inhibitor Cocktail Tablet (Roche Diagnostics, Brussels, Belgium) and 1% tributyl phosphate (TBP) (Sigma-Aldrich, Diegem, Belgium). The cells were suspended in 100 µl of the extraction buffer and homogenized with the Tissue Lyser II (Qiagen, Antwerp, Belgium) and 1.4 mm ceramic beads (Labconsult, Brussels, Belgium). Subsequently, the protein samples were quantified, using the Bicinchoninic Acid (BCA) protein assay kit (Sigma-Aldrich, Diegem, Belgium) according to the manufacturer's instructions with standard protein solutions of 0.125 mg/mL, 0.25 mg/mL, 0.5 mg/mL, 0.75 mg/mL, 1 mg/mL, 1.5 mg/mL and 2 mg/mL (Bio-Rad, Temse, Belgium). The absorbance of the Cu-BCA chelate formed upon addition of protein was measured at 562 nm and normalized at 750 nm using the Nanodrop spectrophotometer (Thermo Scientific, Ghent, Belgium). Twenty µg of sample was mixed with 4x Laemmli buffer (Bio-Rad, Temse, Belgium), Beta-Mercapto-ethanol (Sigma-Aldrich, Diegem, Belgium) (2.5% of the total volume) and MilliQ to get a final volume of 20 µl. Samples were heated at 95°C for 5 minutes and were separated by a vertical 26-well 4-15% (TGX Stain-free Precast Protein Gel, Bio-Rad, Temse, Belgium) sodium-dodecyl-sulfate (SDS) polyacrylamide gel at 300 V for 30 minutes. Thereafter, proteins were transferred onto a nitrocellulose membrane using Trans-Blot Turbo Transfer System (Bio-Rad, Temse, Belgium). The membranes were blocked for 1 hour at room temperature in blocking buffer (5% Non-Fat Dry Milk). Then, membranes were incubated overnight at 4°C with primary antibody (NRF2 Mouse Monoclonal antibody, ABCAM) diluted in blocking buffer (1/1000). The membranes were washed three times for 5 minutes with 1x washing buffer (0.05 M Tris-HCl, 0.15 M NaCl, 0.05% Tween 20, pH 7.4; Component B of the WesternDotTM 625 Western Blot Kit, Invitrogen, Ninove, Belgium). This was followed by addition of diluted secondary antibody 1/1000 times in washing

buffer to the membrane and incubated for 1 hour at room temperature then washing twice with washing buffer and once with 1x PBS. The antibody complexes were visualized usingThe QDot® 625 streptavidin conjugates (Component D of the WesternDotTM 625 Western Blot Kit, Invitrogen, Ninove, Belgium), 1/4000 times diluted in blocking buffer and incubated for 1 hour at room temperature were used to visualize the protein-antibody complexes.

Following washing, protein bands on the membrane were detected by exposure to UV-light using Fusion FX Imager (Vilber Lourmat, Eberhardzell, Germany). The bands were quantified by densitometry using the Bio1D analysis software (Vilber Lourmat, Eberhardzell, Germany). The protein levels were normalized against those of vinculin, which were run on the same membrane as that of the protein of interest.

2.5 ROS ASSESSMENT USING CM-H2DFCDA PROBE

To detect intracellular ROS, 2.2 x10^6 cells were cultured for five days in 75-cm^2 culture flask in medium with iodine. 3 x 10^5 cells/well were transferred to six-well plates for three extra days. On the day of the experiments the medium was replaced with phenol free medium with or without NAI (10^{-8} M). This was followed by irradiation with low, intermediate and high doses of radiation. Each plate corresponded to a single dose and comprised three biological replicates of iodine-deficient thyroid cells and 3 replicates of iodine sufficient thyroid cells. Immediately after irradiation, 10 µmol/L of CM-H2DCFDA dissolved in DMSO (Thermo Scientific, Ghent, Belgium) prepared in HBSS with Ca^{2+} and Mg^{2+} (Thermo Scientific, Ghent, Belgium) was added to each well plate (1/100 dilution in HBSS with Ca^{2+} + Mg^{2+}) and the cells incubated for 45minutes in the dark. The cells were washed and trypsinized by the addition of 500 µl of trypsin (0.05% Trypsin-EDTA) per well followed by incubation for 5 minutes. 1 ml/well of appropriate medium was added to stop trypsinization and cells transferred to a 2ml Eppendorf round bottom tube for centrifugation for 5 minutes at 200 xg. The supernatant was discarded and pellets washed twice with preheated HBSS without Ca^{2+} and Mg^{2+}. The cells were centrifuged for 5 minutes at 200 xg at room temperature and re-suspended in 450 µl of HBSS without Ca^{2+} and Mg^{2+}. Afterward, 50 µl of PI was added to each tube and tubes placed on ice. The contents of the tubes were transferred into filter tubes and centrifuged for a few minutes at 500 rpm and then analyzed by flow cytometry. The cells treated with 20µm Tert-butyl Hydroperoxide (TBHP) were used as a positive control.

2.6 TIME-LAPSE CELL IMAGING ASSAY FOR PROLIFERATION

Cell proliferation following co-treatment of PCCL3 cells was performed with the IncuCyte ZOOM™ live cell imaging system (Essen BioScience, USA). PCCL3 cells were grown for seven days in medium with iodine in 75-cm^2 cell culture flasks. A day before irradiation, cells were transferred to 96-well Costar plates (Corning Life Sciences) at a density of 2 x 10^4 cells/well in 100 µl of medium with iodine. The cells were incubated at 37°C and 95% CO_2 for 24 hours. On the day of the experiments and before irradiations, the medium was replaced with fresh medium with and without iodine. Following irradiation, the cells were placed in the IncuCyte™ Zoom apparatus. The wells were imaged at 10x objective (phase contrast) to obtain two images/well at scanning intervals of 2 hours for 72 hours.

Each experimental condition had six biological replicates (n=6) to increase the statistical power. The IncuCyte integrated software was used to calculate mean object area from non-overlapping bright phase images from various wells. Cell proliferation was expressed as the mean ± standard deviation (SD) of phase object area (μm^2).

2.7 TIME-LAPSE CELL IMAGING ASSAY FOR APOPTOSIS

For apoptosis we used the IncuCyte™ Zoom (Essen Bioscience, USA). To obtain a multiplex way to kinetically measure apoptosis we combined, Cell player 96-well kinetic Caspase-3/7 reagent and Annexin V reagents (Essen Bioscience, USA). The Caspase-3/7 reagent coupled the activated caspase-3/7 recognition motif (DEVD) to a DNA intercalating dye to enable quantification of apoptosis over time. When added to the medium, this inert, non-fluorescent substrate crosses the cell membrane where it is cleaved by activated caspase-3/7, leading to release of DNA dye and green fluorescent staining of nuclear DNA. Each reagent was prepared in accordance with the manufacturer's protocol. PCCL3 cells were seeded in Costar 96-well plate (Corning Life Sciences) at a density of 3 x 104 cells/well in medium. After 24 hours, the medium was replaced with medium with and without iodine followed by X-irradiation. This was followed by addition of 5µm CellPlayer 96-well Kinetic Caspase-3/7 reagent to each well and Annexin V at a final dilution of 1:200. The plates were placed into microplate tray in the IncuCyte™ Zoom in which the caspase activity and the phosphatidylserine externalization (Annexin V) was non-invasively monitored. The wells were imaged at 10x objective to obtain two images/well at scanning intervals of the 2 hours during 72 hours. The caspase-3/7 and Annexin V signals were measured in the green and red channels respectively. The integrated software was used to process and analyze the images. Results were expressed as apoptotic index gotten by dividing the red or green object confluence by phase confluence as determined by the IncuCyte software. Each experimental condition had six biological replicates (n=6) of iodine sufficient and iodine deficient conditions.

2.8 COMET ASSAY FOR DNA DAMAGE ANALYSIS

To investigate DNA damage, we used the comet assay at VITO (Vlaamse Instelling Voor Technologisch Onderzoek) Toxicology laboratory 1. 2.5 x 10^6 cells/well were seeded in 6-well plates in medium with iodine for seven days. On the day of the experiment, the medium is replaced with medium with and without iodine followed by X-irradiation. Following co-treatment cells were immediately kept on ice, washed twice with PBS and harvested by trypsinization and suspended in PBS (1 million cells/ml). 10 µl of cell suspension was mixed with 0.8% low melting point agarose in preheated 1xPBS. This mixture was transferred onto superfrost microscope slides (GelBond®), pre-coated with 1% normal agarose and later with 0.6% normal agarose/PBS. Cover-slips were put on the slides which were kept on ice for 10 minutes. Thereafter, coverslips were removed and slides lysed with a lysis solution (2.5 M NaCl, 100 mM Na2EDTA, 1.2g Tris, 0.1% Triton X-100, 10% DMSO and pH adjusted with NaOH) overnight and in the dark for 24 hours. The slides were washed twice with PBS and then placed in the electrophoresis buffer (300 mM NaOH and 10 mM Na2EDTA in 1000 ml MilliQ water) and denatured for 40 minutes at speed of 22 revolution/minutes. Electrophoresis

was applied at 1V/cm and the Volt was additionally controlled with a portable voltmeter. Following neutralization with cold PBS, the slides were air-dried and stained with SYBR®Gold (SIGMA-Aldrich) overnight. The GelBond® slides were analyzed by Metafer Metacyte version 5 (Metasystems, Germany). A total of 300 comets per condition were analyzed. After rejections of artifacts, the median of the remaining cells per slide was calculated. Three slides per experimental condition were analyzed. The median value of each replicate was calculated for each condition, and from these three slides, the mean value of the dose group was calculated. The positive control cells (PCCL3 and human blood cells) were treated with 20 µl methanesulfonate (EMS) (300 mM). the results are expressed as mean ± standard deviation (SD) of the percentage of DNA tail median.

2.9 STATISTICAL ANALYSIS

Graphpad Prism versions 5 and 7.2 statistical software were used to analyze the results. All experiments were performed with at least three biological replicates. The results are presented as the mean ± Standard deviation (SD). For significant differences between the various iodine status and different radiation doses, a two-way ANOVA was performed followed by a Bonferroni posthoc test. The results were considered statistically significant when $p<0.05$.

3 RESULTS

3.1 RADIATION AND IODINE DEFICIENCY INDUCED OXIDATIVE STRESS

In our preliminary study with PCCL3 cells, we had observed significant oxidative stress (ROS production) following co-treatment of cells with IR and ID. To further investigate or validate the oxidative stress observed, we investigated NRF2 protein expression using western blot which has been reported as a biomarker of oxidative stress. NRF2 highly controls antioxidant response and hence control approximately 200 genes some of which control antioxidant enzymes (81). To investigate NRF2 expression, cells were cultured with and without iodine and exposed to low, intermediate and high doses of radiation. Protein expression level of NRF2 was analyzed by western blot one hour after co-treatment.

We observed a dose-dependent trend of increase in the expression of NRF2 in both iodine sufficient and deficient conditions. In both conditions, the results were significant at 3 Gy (p= 0,0003) and 0.5 Gy (p= 0,0043) as compared to the controls (iodine and iodine deficiency). However, there was no additive effect when the two factors were combined even at high doses (**Figure 3**). This data confirms our preliminary results in FRTL-5 and PCCL3 that IR and ID both induced oxidative stress in thyroid cells at high doses with no additive effect.

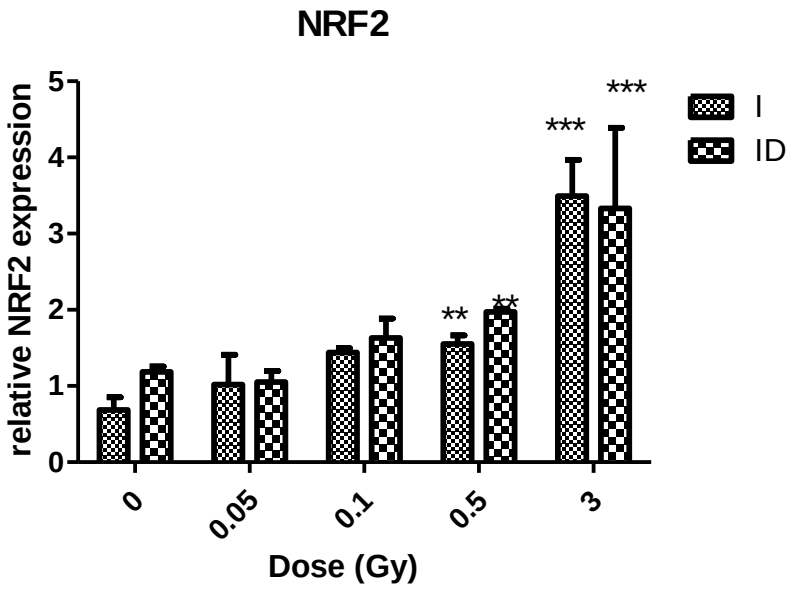

Figure 3: IR and ID induced oxidative stress in a dose-dependent manner. ID and IR-induced significant expression of NRF2 oxidative stress in PCCL3 cells at intermediate and high doses of radiation in both iodine deficient and iodine sufficient conditions (**0.5 Gy, p=0.0043**, **3 Gy, p=0.003**) respectively. The expression is generally higher in iodine-deficient conditions but it is not statistically significant**.** Western blot was used to analyze NRF2 protein expression in PCCL3 cells deprived of iodine and X-irradiated with low, intermediate and high doses of radiation. Densitometric values were normalized against those of vinculin. Results are expressed as the mean fold change relative to non-irradiation, iodine-sufficient or deficient thyroid cells ± standard deviation (SD) of 3 biological replicates (n=3).

3.2 EFFECTS OF IR AND ID ON PCCL3 CELL PROLIFERATION

To investigate the effect of IR and ID on PCCL3 cell proliferation, we used the IncuCyte™ ZOOM live cell imaging system to obtain real-time analysis with no disturbance of cell culture. PCCL3 cells were deprived of iodine and X-irradiated with low, intermediate and high doses of radiation and proliferation monitored for 72 hours in the IncuCyte, (10x objective). The IncuCyte integrated software was used to process the obtained images Each experimental condition had six biological replicates (n=6) of iodine deficient and iodine sufficient conditions.

We noticed co-treatment significantly enhanced PCCL3 cell proliferation in a time-dependent manner ($p<0.001$) (**Figure 4A**). This is demonstrated by phase-contrast images up to 72 hours of incubation at all doses in iodine deficient conditions. The mean phase object area (μm^2) showed that IR and ID had a significant effect on proliferation after 40 hours at all doses compared to the iodine sufficient conditions ($p<0.0001$ for all doses except 3Gy, $p<0.001$) (**Figure 4A and 4B**). Radiation and iodine reduced cell proliferation while iodine deficiency and radiation enhanced cell proliferation at all doses especially at 0 Gy and 3 Gy compared to respective doses (**Figure 4C and 4G**). This proliferation is actually associated with iodine deficiency as we observed enhanced proliferation in iodine-deprived control compared to iodine sufficient control. The highest proliferation is observed at low doses compared to the control in both conditions and this could be attributed to hormesis. We equally observed that ID alone enhanced proliferation with no radiation compared to iodine sufficient conditions. However,it was more enhanced (synergistically) when combined with IR especially at low doses as mentioned above (**Figure 4C 4D 4E 4F and 4G**). Taken together, these data indicates that the cells survived or resist possible IR and ID induced damage and continue to proliferate.

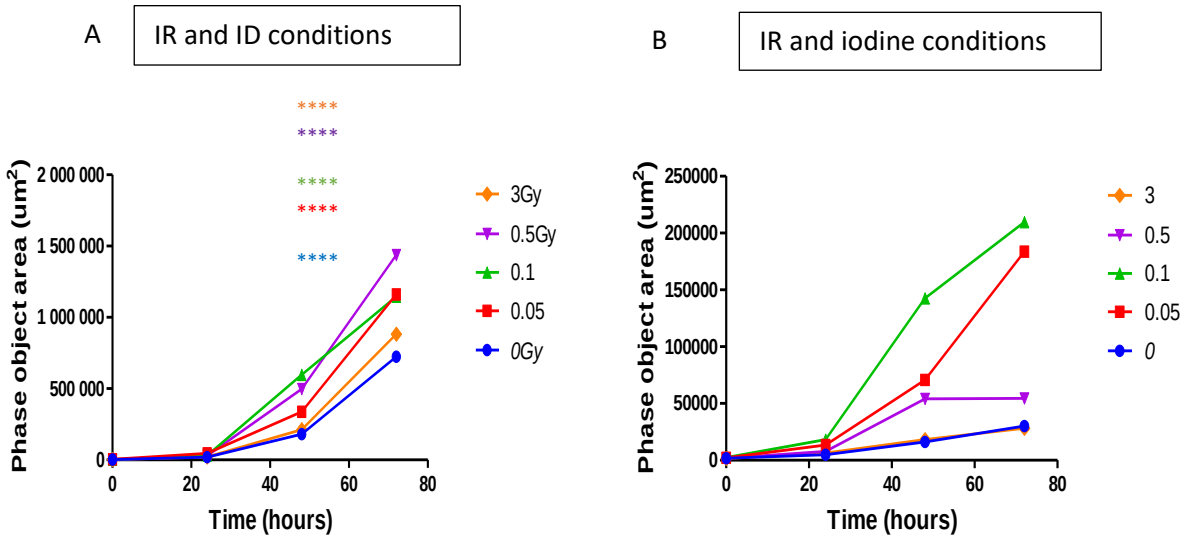

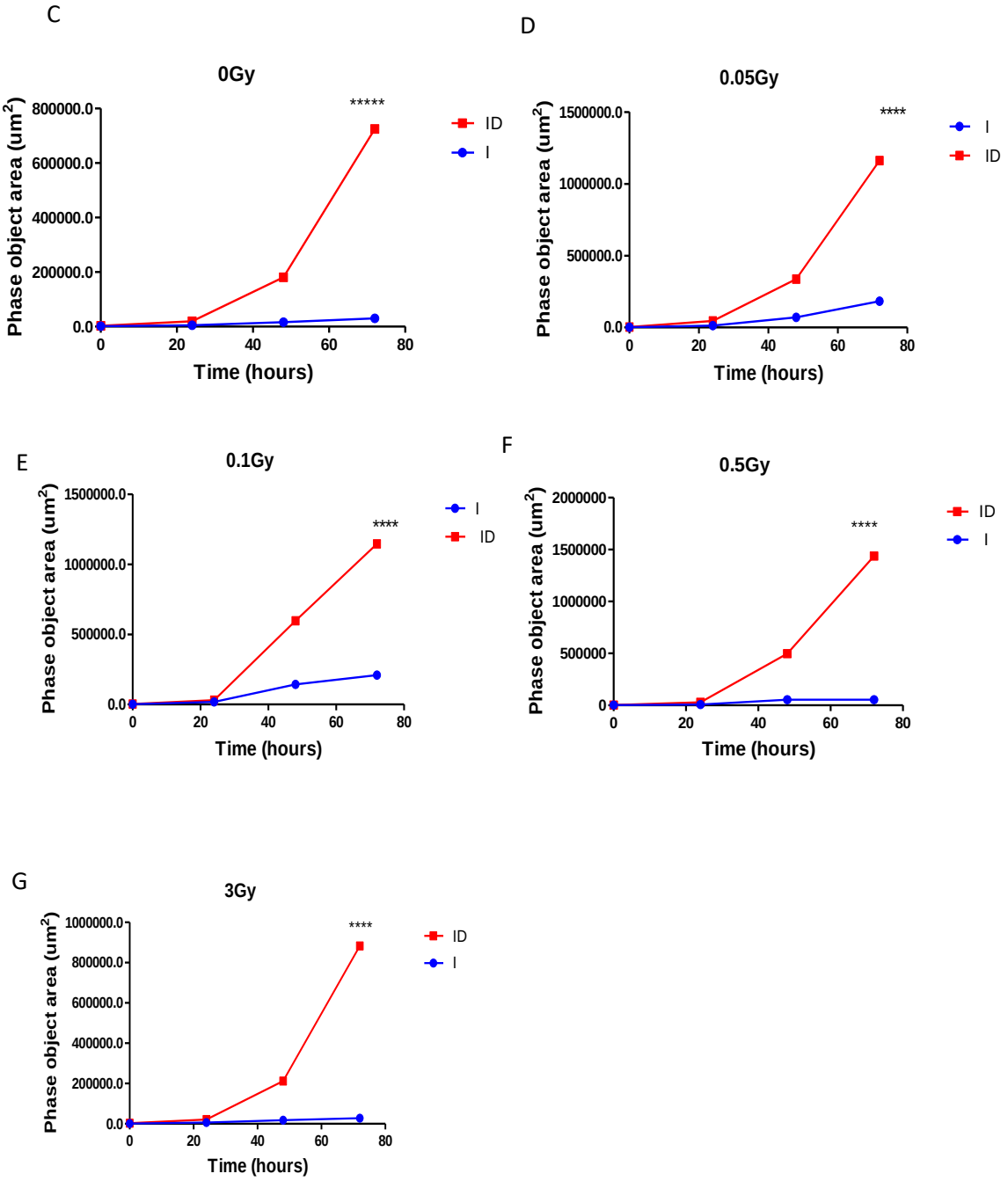

Figure 4: Effects of ID and IR on cell proliferation as measured by IncuCyte™ Zoom live cell imaging system: (A) ID and IR significantly enhanced cell proliferation at all doses especially at low doses of radiation. Iodine deficiency and radiation enhanced proliferation of PCCL3 cells at all doses while iodine sufficient slowed down proliferation (**B**). **(C)** 0Gy **(D)** 0.05Gy, **(E)** 0.1Gy, **(F)** 0.5Gy, **(G)** 3Gy had enhanced proliferation when deprived of iodine. Proliferation is expressed as mean phase object area for each time point. **** indicates significant difference ($p < 0.0001$) between iodine deficient condition when compared to the iodine sufficient condition of the same dose. Results are expressed mean ± standard deviation of object confluence area (μm^2).

3.3 EFFECTS OF RADIATION AND IODINE DEFICIENCY ON DNA DAMAGE

In our preliminary results, we observed that IR and ID induced DNA damage in FRTL5 cells. However, no additive effect was observed. To confirm this DNA damage induced by the co-treatment of IR and

ID, the comet assay was used to analyze DNA damage in PCCL3 cells. The IR and ID co-treated cells were embedded in agarose and spread on microscope slides. These were lysed overnight followed by denaturation, electrophoresis then staining. The DNA which is negatively charged at PH > 13 migrated to the positive pole and the damaged DNA formed a comet shape. The intensity of the comet (damaged DNA) tail was detected by Metafer software version 5. Each experimental condition had three biological replicates. Results are expressed as mean ± standard deviation (SD) of percentage of DNA tail median

We observed IR and ID did not induced DNA damage irrespective of iodine status compared to the controls (p= 0,9999) (**Figure 5A and B**). Posthoc testing equally did not reveal any significant difference related to the iodine status and this is for all doses. For our positive control, cells were treated with Ethyl methanesulfonate (EMS) to induce DNA damage but equally had no significant effect (p > 0.05). However, we noted that EMS significantly induced DNA damage when added to human blood cells (p<0.0001). Taken together, this data is contrary to that observed in FRTL5 cell lines in which ID and IR-induced significant damage as from intermediate dose of 0.5 Gy. This indicates PCCL3 cells are very resistant to the double stress of ID and IR as no DNA damage is observed in these cells even with the addition of EMS.

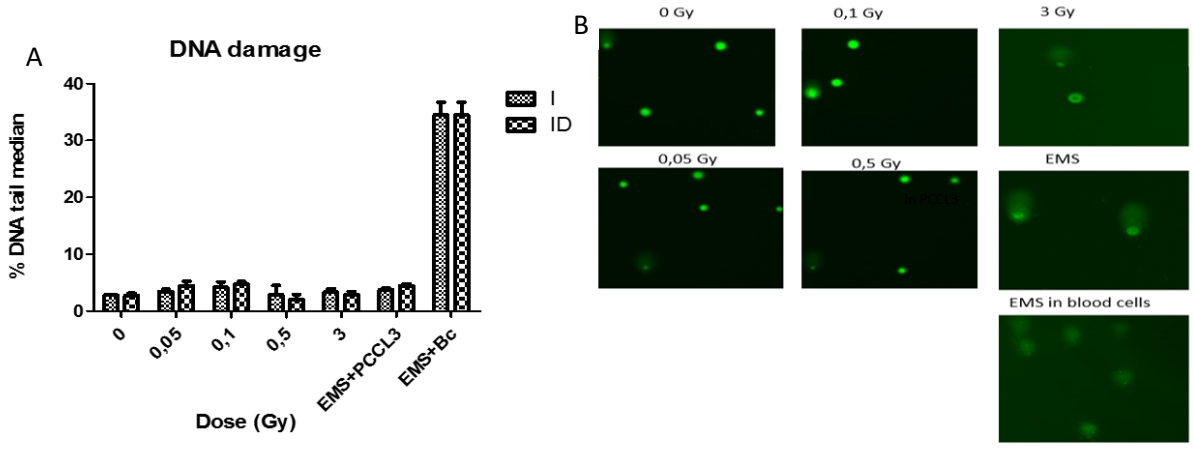

Figure 5: Effects of ID and IR on DNA damage. (A) ID and IR did not significantly induce DNA damage in PCCL3 cells. DNA damage was investigated using the comet assay. Results are expressed as mean percentage DNA tail median ± standard deviation (SD). **(B)** Comet tails indicating DNA damage under various iodine conditions and at different doses. *** signifies p<0.0001 and EMS are the positive controls, Bc= blood cells.

3.4 EFFECTS OF IONIZING RADIATION AND IODINE DEFICIENCY ON APOPTOSIS

To evaluate apoptosis in PCCL3 cells co-treated with ID and IR, we performed an Annexin V and Caspase-3/7 multiplex apoptotic assay using the IncuCyte™ Zoom. Following co-treatment of PCCL3 cells, which were grown in 96 well plates, the Annexin V and caspase-3/7 were added and thereafter the plates were placed in the IncuCyte and monitored for 72 hours. Two phase-contrast and red and

green fluorescent images of the same optic field were automatically taken every two hours (**Figure 5B**). Each experimental condition seen on the figures had six biological replicates each (n=6). Apoptotic index was obtained by dividing fluorescent (red or green) object confluence(%) against phase object confluence. Unfortunately, the caspase staining did not work.

48 hours following co-treatment, we observed a significant increase in apoptotic cells at high dose (3 Gy) irrespective of iodine status ($p< 0.01$) with respect to the control conditions. At intermediate dose (0.5 Gy), we equally observed a significant increase in cell death ($p<0.01$) iodine deficient conditions ($p<0.01$) with respect to the controls. We equally observed a general dose-dependent trend increase in apoptosis in all conditions irrespective of iodine status compared to the control (iodine sufficient) ($p<0.0001$) (**Figure 6A** and **B**).

72 hours after co-treatment of cells with IR and ID, we observed a significant increase in apoptosis with respect to irradiation irrespective of iodine status ($p<0.0001$) (**Figure 6C**). At all doses, we observed significant cell death compared to the respective controls sham irradiated (**Table 1**) for low, intermediate and high doses of radiation. Nonetheless, we did not observe any additive effect with IR and ID.

This observation, suggest radiation and ID induced apoptosis in a dose and time-dependent manner as even lower doses induced apoptosis significantly after 72 hours. However, we noted that these cells are resistant to low dose and IR and at an earlier time point as there was no significant cell death as these doses after 48 hours. After 72 hours the cells continue to proliferate suggesting the apoptosis is not sufficient to stop cell division.

Table 1: Table of significance of IR and ID induced apoptosis 72 hours post co-treatment showing significant differences in apoptosis between various radiation doses and iodine status

Iodine			Iodine deficiency		
comparisons	significance	p-value	comparisons	significance	p-value
0 Gy vs 0.05 Gy	ns	>0.9999	0 Gy vs 0.05 Gy	ns	>0.9999
0 Gy vs 0.1 Gy	ns	>0.9999	0 Gy vs 0.1 Gy	ns	>0.9999
0 Gy vs 0.5 Gy	***	<0.001	0 Gy vs 0.5 Gy	****	<0.0001
0 Gy vs 3 Gy	****	<0.0001	0 Gy vs 3 Gy	****	<0.0001
0.05Gy vs 0.1 Gy	ns	>0.9999	0.05Gy vs 0.1 Gy	ns	>0.9999
0.05Gy vs 0.5 Gy	***	0.003	0.05Gy vs 0.5 Gy	****	<0.0001

0.05Gy vs 3 Gy	**	0,0065	0.05Gy vs 3 Gy	****	<0001
0.1 Gy vs 0.5 Gy	**	0.0051	0.1 Gy vs 0.5 Gy	***	0,0005
0.1 Gy vs 3 Gy	****	0.0001	0.1 Gy vs 3 Gy	***	0,0001
0.5 Gy vs 3 Gy	*	0,0145	0.5 Gy vs 3 Gy	ns	0,0666

A

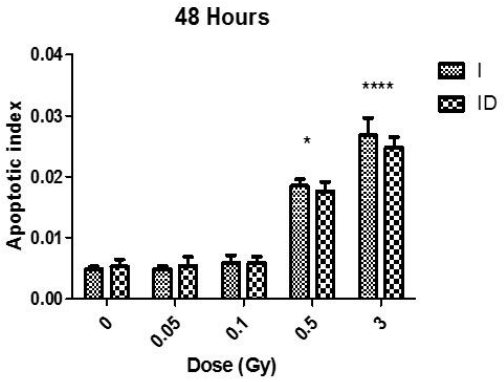

B

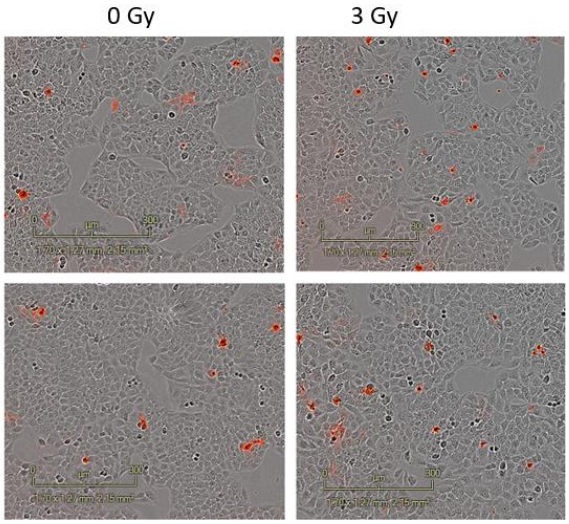

C

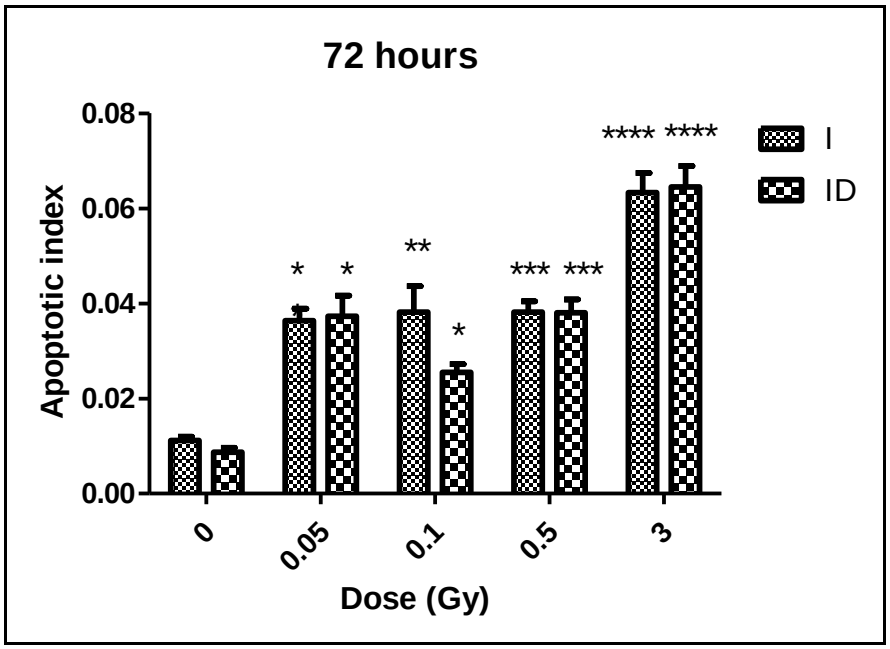

D

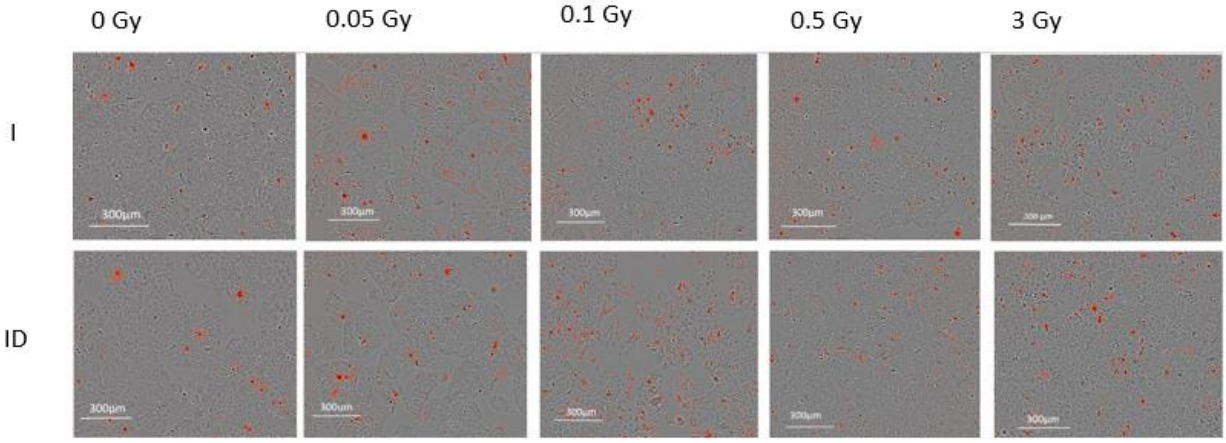

Figure 6: Radiation and Iodine deficiency induced apoptosis in PCCL3 cells. (A) IR and ID induced apoptosis 48 hours post co-treatment with IR and ID which is significant at 0.5 Gy and 3 Gy irrespective of iodine status. **(B)** The red staining in the images represent the dead cells after 48 hours **(C)** IR and ID induced apoptosis 72 hours post co-treatment with IR and ID which is significant at all the doses irrespective of iodine status. Results are expressed as mean apoptotic index ±SD which represents a ratio of Annexin V object confluence and total object confluence. **(D)** Representative images of Annexin V positive cells for each dose obtained from IncuCyte™ Zoom live cell imaging after 72 hours. * indicates significant difference with respect to the controls irrespective of iodine status.

3.5 RADIATION AND IODINE DEFICIENCY INDUCED ANTI-APOPTOTIC GENE EXPRESSION

To investigate the resistance to apoptosis and the enhanced proliferation, anti-apoptotic genes were investigated. The mRNA expression level of B-Cell Lymphoma 2 (Bcl-2) and Myeloid Leukemia Cell

Differentiation Protein (Mcl-1) were evaluated 24 hours following iodine deprivation and irradiation. PCCL3 cells were cultured with and without iodine and irradiated with low, intermediate and high doses of radiation. mRNA expression level of Bcl-2 and Mcl-1 were evaluated by RT-qPCR after 24 hours. Each experimental condition had three biological replicates (n=3).

Radiation had an overall dose-dependent increase in Bcl-2 mRNA expression 24 hours post co-treatment and this increase was significant at 3Gy (p<0,0001) (**Figure 7A**). Posthoc analysis clearly identified significant differences between each iodine condition and high dose (p= 0,0292, p=0,0092 for 3 Gy iodine and iodine deficiency respectively) (**Table 2**). However, we observed no significant differences observed between iodine deficient cells compared to iodine sufficient conditions, hence no synergistic effect.

We equally observed a significant effect in a dose-dependent manner in the expression of Mcl-1 (p=0.0303), however, no synergistic effect was observed between iodine deficient or iodine sufficient conditions (**Figure 7B**). Despite that, the posthoc analysis did not reveal specific significance between various doses compared to the controls. We equally noted that co-treatment had an additive negative effect at all doses though none was statistically significant.

This data seems to suggest the resistance we observed with respect to apoptosis could be due to upregulation of these antiapoptotic genes. This is important as Bcl-2 is prevents the disruption of membrane potential by inhibition of cytochrome c. Mcl-1 has been shown to be vital for the survival of many cell lineages and is the most amplified genes in cancer, however, the mechanism for enhanced survival of normal and cancerous cells is unknown.

Table 2: Table of significance of Bcl-2 expression 24 hours post iodine deficiency and radiation treatment showing changes in expression between various radiation doses and iodine status.

Iodine			Iodine deficiency		
comparisons	significance	p-value	comparisons	significance	p-value
0 Gy vs 0.05 Gy	ns	>0.9999	0 Gy vs 0.05 Gy	ns	>0.9999
0 Gy vs 0.1 Gy	ns	>0.9999	0 Gy vs 0.1 Gy	ns	>0.9999
0 Gy vs 0.5 Gy	ns	>0.9999	0 Gy vs 0.5 Gy	ns	>0.9999
0 Gy vs 3 Gy	*	0,0292	0 Gy vs 3 Gy	**	0,0092
0.05Gy vs 0.1 Gy	ns	>0.9999	0.05Gy vs 0.1 Gy	ns	>0.9999
0.05Gy vs 0.5 Gy	*	0,0436	0.05Gy vs 0.5 Gy	ns	0,0603

0.05Gy vs 3 Gy	**	0,0065	0.05Gy vs 3 Gy	**	0,0065
0.1 Gy vs 0.5 Gy	ns	>0.9999	0.1 Gy vs 0.5 Gy	ns	>0.9999
0.1 Gy vs 3 Gy	**	0,0087	0.1 Gy vs 3 Gy	**	0,0067
0.5 Gy vs 3 Gy	ns	0,0754	0.5 Gy vs 3 Gy	ns	0,1130

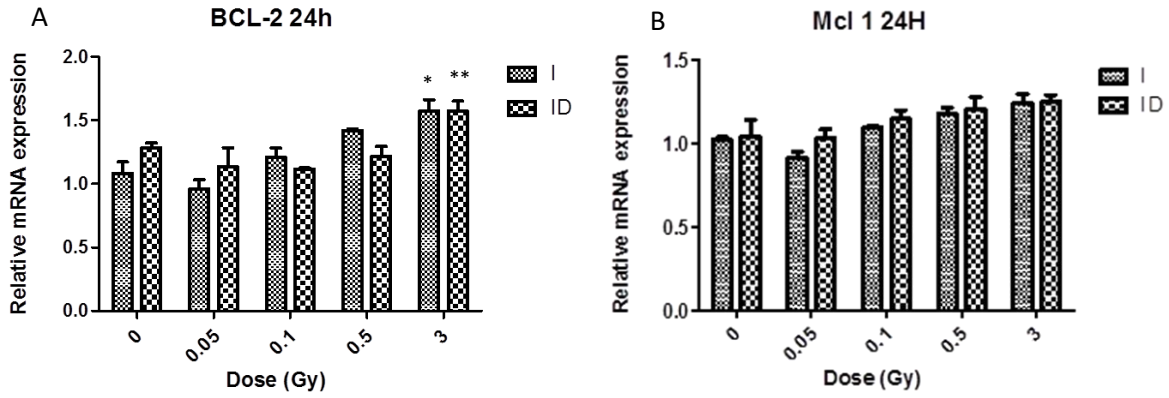

Figure 7: ID and IR significantly enhanced anti-apoptotic gene expression Bcl-2 (p<0,0001) and Mcl-1 (p=0,0303) after 24 hours. (A) Bcl-2 **(B)** Mcl-1 mRNA expression is dose dependent but there are no significant differences between iodine deficient and iodine sufficient conditions. mRNA expression was analyzed by RT-qPCR after PCCL3 cells were cultured 24 hours without iodine and exposed to low, intermediate and high radiation doses. Results are expressed as mean fold change ± standard deviation (SD) and normalized against β-actin.

3.6 EFFECTS OF RADIATION AND IODINE DEFICIENCY ON DNA REPAIR MARKERS

Ataxia-Telangiectasia Mutated (ATM) serine/threonine and RAD50 double strand break repair protein have been demonstrated to be activated during double-strand breaks (DSBs) to enable phosphorylation of key genes vital in DNA repair, cell cycle checkpoint and apoptosis. To confirm the results of the comet assay, (DSBs) associated with the treatment of cells with IR and ID, we evaluated these DNA damage repair genes in PCCL3 cells. The PCCL3 cells were cultured without iodine deficiency and irradiated with low, intermediate and high doses of radiation. This was followed by RT-qPCR with three biological replicates representing each experimental condition. IR and ID had no significant effect on the ATM mRNA expression levels 24 hours post treatment (p=0,7949). This

was expected as we observed no significant DNA damage after co-treatment (**Figure 8A**). we equally did not observe any additive effect with combined treatment. Co-treatment had overall dose-dependent significant effect on RAD50 mRNA expression ($p<0.0001$) . Post hoc analysis revealed radiation had an overall significant effect ($p=0,0023$) . We observed a dose-dependent additive expression of RAD50 which is significant at 3 Gy ($p < 0.05$) compared to all the controls and could possibly be responsible for the DNA repair (**Figure 8B**). Taken together, this data suggest DNA repair occur and is responsible for the absence of significant DNA damage even at high dose in PCCL3 is through the RAD50 dependent DNA repair pathway (MRN).

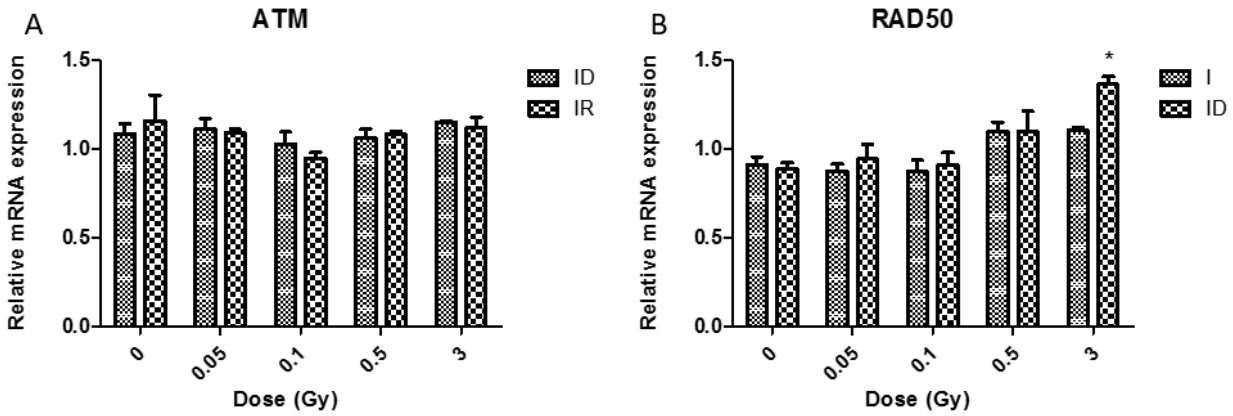

Figure 8: Effects of ID and IR DNA repair markers 24 hours after co-treatment. (A) IR and ID had no overall significant effect on ATM mRNA expression (**p=0,7949**). **(B)** IR and ID had an overall significant effect on RAD50 mRNA expression (**p=<0.0001**) and had an additive negative effect at 3Gy (**p<0.05**). mRNA expression was analyzed by RT-qPCR after PCCL3 cells were cultured 24 hours without iodine and exposed to low, intermediate and high radiation doses. Results are expressed as mean fold change ± standard deviation (SD) and normalized b against β-actin.

3.7 EFFECTS OF RADIATION AND IODINE DEFICIENCY ON PROLIFERATION AND SURVIVAL SIGNALING PATHWAYS

3.7.1 JAK/STAT SIGNALING PATHWAY

Radiation is known to activate the precancerous JAK/STAT signaling pathway. The activation of STAT3 has been demonstrated in the majority of thyroid cancers especially papillary thyroid cancer (60%) (79). To investigate the effects of co-treatment with IR and ID on JAK/STAT pathway, the levels of STAT3 mRNA expression was evaluated at different time intervals. PCCL3 cells were cultured with and without iodine and irradiated with low, intermediate and high doses of radiation. mRNA expression level of STAT3 was evaluated by RT-qPCR after 24 hours.

The mRNA expression of STAT3 had generally dose-dependent trend with respect to radiation. IR and ID had a similar trend at low doses but not high doses and was not significantly different ($p=0,2584$) after 24 hours compared to the control without iodine (**Figure 9**). However, none was statistically significant. This data suggest STAT3 may likely not be activated by co-treatment and this is contrary to results in FRTL-5, rat thyroid cells in which high dose radiation (3 Gy) activated the JAK/STAT pathway.

To increase the chance of a significant effect by IR and ID, we suggest that the mRNA expression of STAT3 be performed at different time intervals particularly at 48 and 72 hours. Also, the number of replicates should be increased to six to increase statistical power.

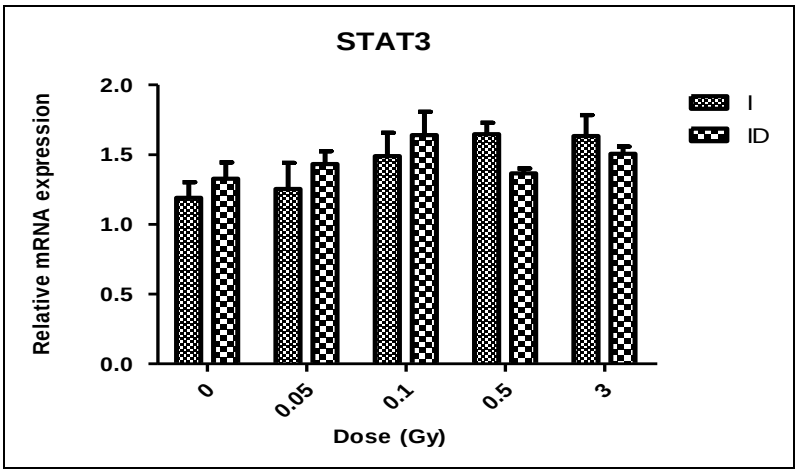

Figure 9: ID and IR co-treatment did not significantly activate JAK/STAT3 signaling pathway at 24 hours (p=0,2584). PCCL3 cells were deprived of iodine for 24 hours and irradiated with low, intermediate and high radiation doses. mRNA expression was analyzed by RT-qPCR at 24 hours after co-treatment of cells with ID and low, intermediate and high radiation doses. The values were normalized against those of β-actin. The results are expressed as mean fold change relative to non-irradiation, iodine sufficient thyrocytes ± standard deviation (SD) of three biological replicates (n=3)**.**

3.7.2 PI3K/AKT1 SIGNALING PATHWAY

DNA damage and oxidative stress from IR has been reported to alter the PI3K/AKT signaling pathway vital in cellular proliferation and survival. To examine changes in the PI3K/AKT signaling pathway upon co-treatment with IR and ID, PCCL3 cells were cultured in iodine deficient and iodine sufficient conditions and exposed to low, intermediate and high radiation doses. AKT1 mRNA expression was analyzed by RT-qPCR from mRNA samples extracted 24 hours after irradiation. Each experimental condition had three replicates (n=3). We observed a significant general dose-dependent expression of AKT1 mRNA 24 hours post treatment (p=0,0292) (**Figure 10**). Nevertheless, posthoc analysis did not reveal significant differences between specific experimental conditions. However, we notice no additive effect at all doses of radiation deprived of iodine. This is contrary to our preliminary data on PCCL3 cells in which co-treatment failed to activate this pathway at the protein level in all conditions. This data suggest co-treatment activates the survival and proliferation (PI3K/AKT pathway) at the level of mRNA 24 hours after treatment and could responsible for the activation observed

Increasing the number of replicates and investigating AKT1 mRNA expression at multiple time intervals will probably increase the chances of observing a significant effect between experimental conditions.

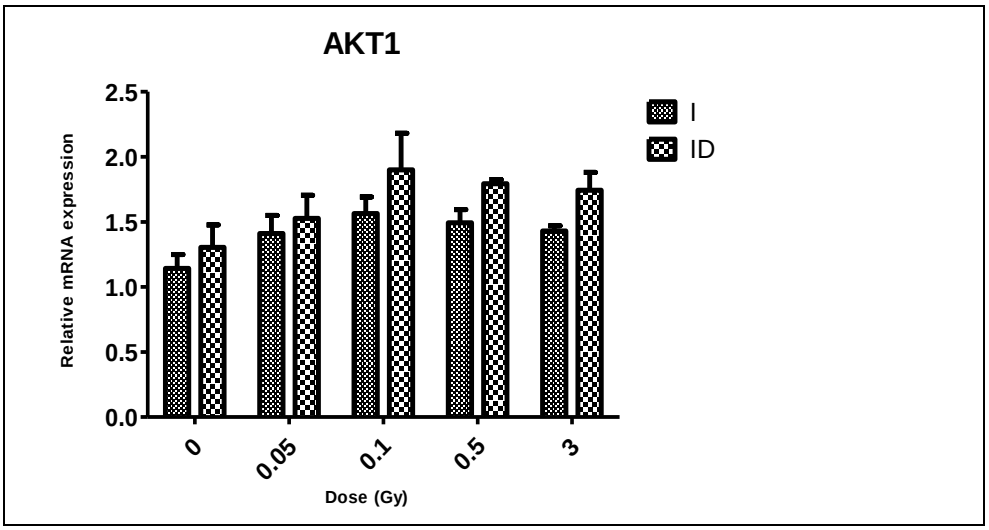

Figure 10: IR had an overall significant effect on AKT1 expression 24 hours following exposure analyzed by RT-qPCR (p= 0,0292). PCCL3 cells that were iodine-deprived for 24 hours and irradiated with low, intermediate and high radiation doses. mRNA expression analyzed by RT-qPCR. Results are expressed the mean of the relative fold change ± standard deviation (SD) of three biological replicates (n=3) in each experimental conditions.

3.7.3 RADIATION AND IODINE DEFICIENCY ACTIVATES CELL CYCLE REGULATOR CYCLIN D2

Cyclin D2 (CCND2) has been implicated in processes such as cell cycle control and proliferation and oncogenic transformation this is because cell lines expressing CCND2 have been associated with invasive behavior . High expression of cyclin D2 is reportedly frequent in follicular thyroid cancers and this is downstream of the Pituitary Homeobox 2 (PITX)/Cyclin D (CCND2) pathway a downstream pathway of β-catenin. So to investigate the effects of ID and IR in CCND2 activation, PCCL cells were deprived of iodine followed by irradiation with low, intermediate and high doses of radiation. mRNA levels were measured by RT-qPCR 24H post treatment. Each experimental condition had three biological replicates (n=3).

As expected, 24 hours after co-treatment, IR and ID significantly induced CCND2 mRNA expression in a dose-dependent manner as from 0.05 Gy in both iodine-deprived and sufficient conditions ($p<0.0001$). However, we did not observe any additive effect when ID and IR were combined at any dose compared to IR and iodine. However, we noted significance at 3 Gy with ID compared to the 0 Gy, 0.05Gy and 0.1Gy with ID (**Figure 11**) (**Table 3**). This data shows PCCL3 cells may regulate their cell cycle control via the upregulation of CCND2.

To increase significance between iodine sufficient and iodine condition, we suggest that the number of replicates is increased and also expression investigated at different time intervals such as 48 and 72 hours.

Table 3: Table of significance of CCND2 expression 24 hours post Ionizing radiation treatment showing changes in differential expression between various radiation doses and iodine status (* significance difference)

Iodine			Iodine deficiency		
comparisons	significance	p-value	comparisons	significance	p-value
0 Gy vs 0.05 Gy	ns	>0.9999	0 Gy vs 0.05 Gy	ns	>0.9999
0 Gy vs 0.1 Gy	ns	>0.9999	0 Gy vs 0.1 Gy	ns	0,0949
0 Gy vs 0.5 Gy	ns	0,6662	0 Gy vs 0.5 Gy	ns	>0.9999
0 Gy vs 3 Gy	*	0,0150	0 Gy vs 3 Gy	ns	0,1096
0.05Gy vs 0.1 Gy	ns	>0.9999	0.05Gy vs 0.1 Gy	ns	>0.9999
0.05Gy vs 0.5 Gy	ns	0,1794	0.05Gy vs 0.5 Gy	ns	0,1268
0.05Gy vs 3 Gy	**	0,0058	0.05Gy vs 3 Gy	*	0,0144
0.1 Gy vs 0.5 Gy	ns	>0.9999	0.1 Gy vs 0.5 Gy	ns	0,1268
0.1 Gy vs 3 Gy	ns	0,0823	0.1 Gy vs 3 Gy	***	0,0010
0.5 Gy vs 3 Gy	ns	0,9259	0.5 Gy vs 3 Gy	ns	0,0823

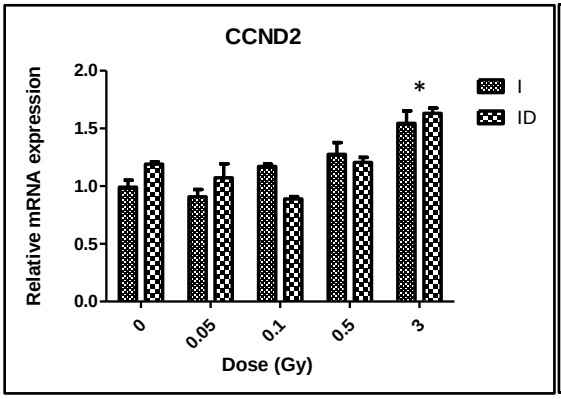

Figure 11: IR induced significant expression of Cyclin D2 24 hours post treatment ($p<0.0001$). PCCL3 cells were iodine deprived and irradiated with low, intermediate and high radiation doses. mRNA expression was investigated after 24 hours and was analyzed by RT-qPCR. Results are expressed a smean of the relative fold change ± standard deviation (SD) of three biological replicates (n=3).

3.8 ANTIOXIDANT CAPACITY

We observed from our comet assay that PCCL3 cells are very radioresistant to DNA damage following co-treatment with irradiation and iodine deficiency. Equally, PCCL3 cells only exhibited significant apoptosis at all doses after 72 hours of exposure to high dose radiation but continue to proliferate.

The ability of PCCL3 cells to resist DNA damage from oxidative stress could possibly be by upregulation of antioxidant genes. We therefore, investigated the antioxidant capacity of PCCL3 cells post co-treatment. This was by measuring mRNA levels of antioxidant genes such as CAT, PRDX5 and NAD(P)H Quinone Oxidoreductase 1 (NQO1). PCCL3 cells were cultured with and without iodine and exposed to low, intermediate and high doses of radiation. mRNA expression level of PRDX5, CAT and NQO1 were analyzed by RT-qPCR at 6 and 24 hours after treatment.

For **PDRX5** expression after 6 hours, we observed no differential expression in mRNA expression in both iodine deficient and iodine sufficient conditions (p=0.3385). We equally observed no differences in iodine deficient and iodine sufficient conditions but strangely for the control and 3 Gy though this is not significant. 24 hours following co-treatment we observed an overall significant dose-dependent expression of PRDX mRNA expression with respect to radiation (p=0.0411). Despite this, the posthoc analysis did not reveal individual significance between conditions. Iodine deficiency had no significant effect on expression of PRDX5 (p=0,8760). We equally observed no significant additive effect at both time intervals (**Figure 12A**).

For **CAT** mRNA expression, there is a trend towards dose-dependent expression 6 hours after co-treatment though this was not statistically significant (p=0,3096). We equally noted a higher expression with IR and ID at all doses except for the intermediate dose though none was significant (p=0,6747). After 24 hours, IR and ID induced a general trend of dose-dependent expression of catalase mRNA expression but this was significant in both iodine deficient and iodine sufficient conditions (p=0.2663) (**Figure 12B**).

For **NQO1** expression, at 6 hours there was a general dose significant expression with respect to radiation (p=0.0449) in iodine supplemented conditions compared to the control iodine. ID and IR had no additive effect on expression. 24 hours after co-treatment, there is a dose-dependent increase expression in NQO1 mRNA expression, however, this is not significant (p=0.1905) (**Figure 12C**). At lower doses we find a slight additive effect in the absence of iodine while there is the absence of additive effect as from intermediate effect after 24 hours.

Taken together, the data suggests that PCCL3 cells exhibit a high antioxidant capacity, which depends on PRDX5 and NQO1 expression. We cannot ignore the high standard deviations we observed with this results as these might have downplayed on the significance. So, we suggest that the sample size for each experimental condition be increased and also expression investigated at different time intervals and also at the protein level.

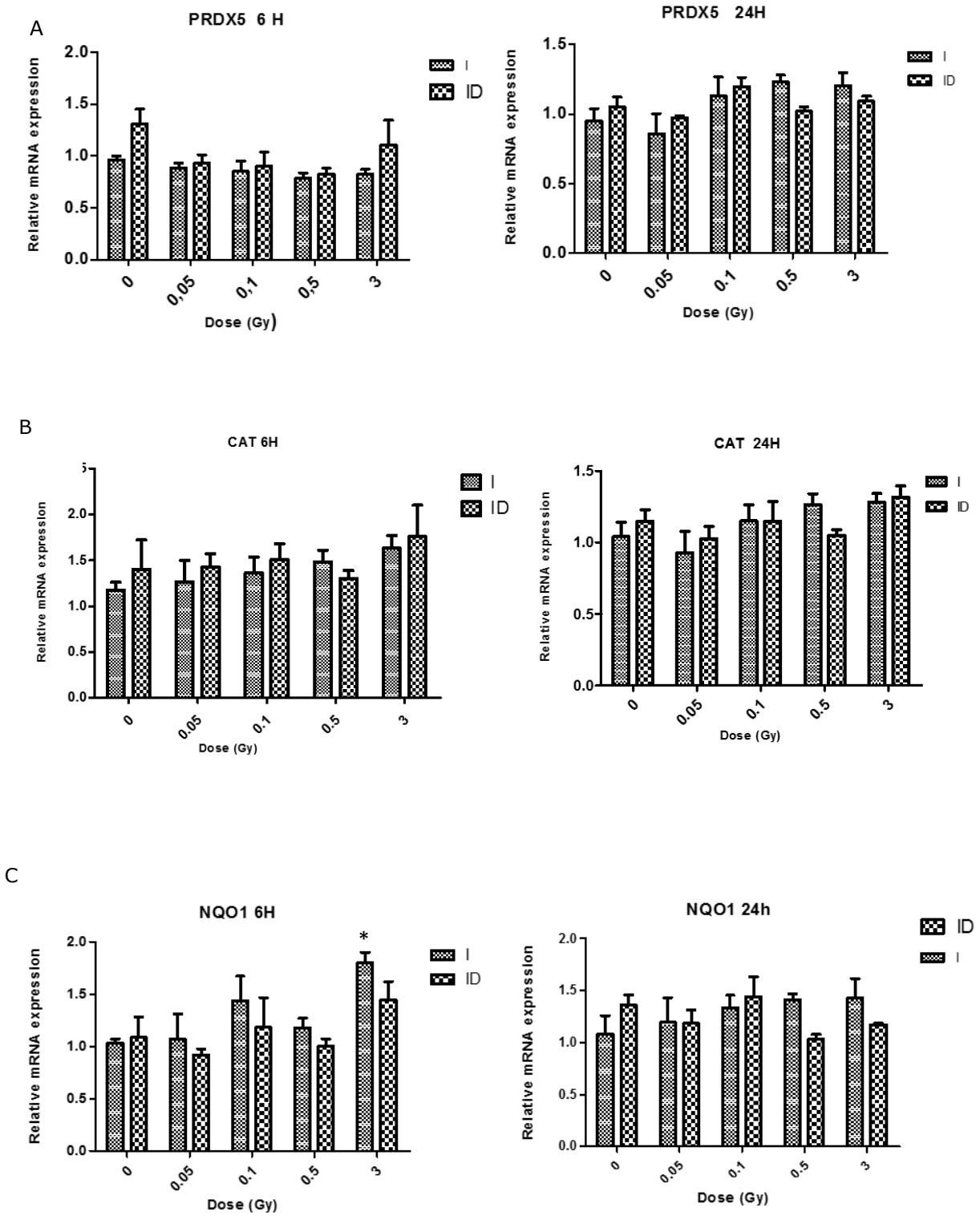

Figure 12: Effect of ID and IR on antioxidant gene expression. **(A)** Radiation had an overall significant increase in PRDX mRNA expression (p=0.0411) at 24 hours but not 6 hours. **(B)** Catalase expression is highly dependent on the dose in both Iodine deficient and iodine sufficient conditions. At 6 hours and 24 hours there is a higher expression of catalase in iodine-deficient conditions however, this is not statistically significant

(**p=0.3385**). **(C)** NQ01, there is a general dose-dependent increased in expression with respect to radiation (**p=0.0449**) 6 hours but not at 24 hours. This increase is higher in iodine deficient condition compared to iodine sufficient conditions. mRNA expression was analyzed by RT-qPCR at 6 and 24 hours after co-treatment of cells with ID and low, intermediate and high radiation doses. The values were normalized using B-actin. The results are expressed as mean fold change relative to non-irradiation, iodine sufficient thyrocytes ± standard deviation (SD) of three biological replicates (n=3

3.9 EFFECTS OF CO-TREATMENT ON CLIP2, A DOSE DEPENDENT THYROID CANCER BIOMARKER

Increased in CAP-Gly Domain Containing Linker Protein 2 (CLIP2) mRNA overexpression has been associated in a dose-dependent manner with PTC following studies after the Chernobyl nuclear disaster. This CLIP2 overexpression has been suggested to play a role in thyroid carcinogenesis via apoptosis, genomic vulnerability and MAPK signaling. Hence to investigate the effects of IR and ID on CLIP2 mRNA expression, PCCL3 cells were cultured with and without iodine and exposed to low, intermediate and high doses of radiation. mRNA expression level CLIP2 were analyzed by RT-qPCR at 24 and 72 hours after treatment.

24 hours post co-treatment, as expected we observed a general dose-dependent trend in the expression of CLIP2 mRNA expression with respect to radiation though it was not significant (p=0,3334). Iodine deficiency equally had no overall significant effect on CLIP2 mRNA expression as we observed no differential expression between the two iodine status (p=0,9071). Combined treatment did not enhance expression as well (p=0,1292) (**Figure 13A**). 72 hours post-treatment we observed no differential expression in CLIP2 mRNA expression with respect to IR and ID (p= 0,2589, p=0,5761 respectively). We equally observed no additive effect or dose-dependent trend in combined treatment which was not significant (p=0,8235) (**Figure 13B**).

CLIP2 is a tumorigenesis marker of which expression is expected to be radiation-dependent but in our system of non-cancerous cells the dose dependency is not observed. So for CLIP2 to be expressed we certainly need to have a cancer context. Hence, CLIP2 expression is more linked to cancer than to radiation. It is not induced only by radiation as demonstrated by our data.

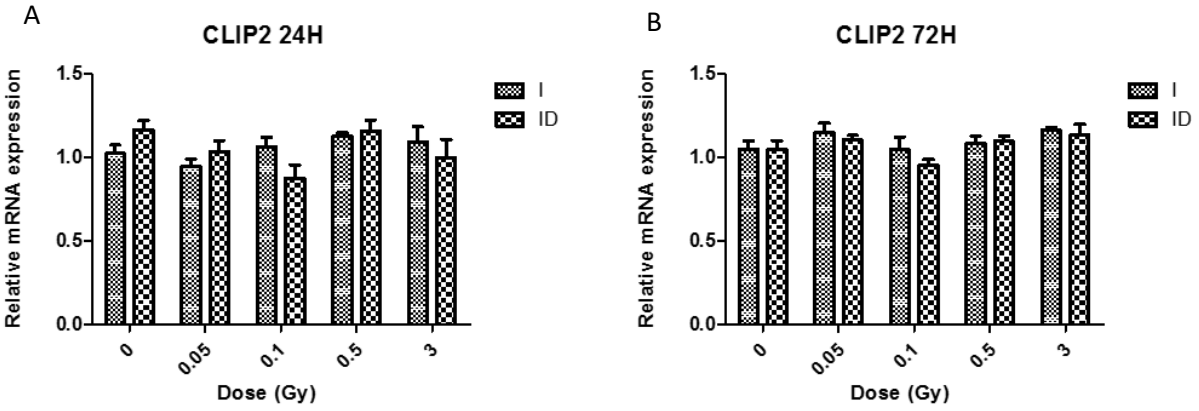

Figure 13: IR and ID had no effect on CLIP2 expression. (A) 24 hours after co-treatment we observed a dose-dependent expression of CLIP2 mRNA but this is not significant **(**p=0,3334). **(B)** IR and ID had no effect on differential expression of CLIP mRNA. mRNA expression was analyzed by RT-qPCR at 6 and 24 hours after co-treatment of cells with ID and low, intermediate and high radiation doses. The values were normalized against those of B-actin. The results are expressed as mean fold change relative to non-irradiation, iodine sufficient /deficient conditions thyrocytes ± standard deviation (SD) of three biological replicates (n=3)

4 DISCUSSION AND OUTLOOK

The incidence of thyroid cancer is on the rise globally. This increasing incidence is largely attributed to increase in screening and advances in diagnostic technologies which can detect very small tumors unlike before. Equally, the population is increasingly being exposed to ionizing radiation from medical and industrial applications. Furthermore, two billion people suffer from iodine deficiency globally which is associated with many pathologies such as goiter, thyroiditis and Grave disease. This is because ID and IR are two risk factors that are capable of influencing thyroid carcinogenesis. The Chernobyl accident was followed by a high incidence of thyroid cancer in exposed areas compared to known areas. It was equally noticed that incidence was much higher in iodine deficient areas compared to iodine sufficient areas. Despite this, there have been no studies so far to the best of our knowledge, which investigated the mechanisms of the combined effects of low dose IR and ID at the cellular and molecular level on normal thyrocytes exposed to IR and ID. Therefore, the necessity of our present study.

The **objective** of this study was to investigate the cellular and molecular effects of low dose IR and iodine deficiency on normal thyroid cells (PCCL3). In our group, we had performed previous experiments on FRTL5 cells and some on PCCL3 in which ROS production (oxidative stress) was observed. So, in this project, we compared the results obtained with FRTL5 and validated our preliminary results in PCCL3. This was by further assessing on PCCL3 cells exposed to IR and ID the following: oxidative stress, DNA damage, DNA repair, proliferation and apoptosis. We equally investigated gene expression changes vital to antioxidant defense, anti-apoptotic, survival and proliferation signaling pathways as well as radiation responsive elements.

Oxidative stress that results from exposure to ionizing radiation has been known to cause DNA and cellular damages and also initiate apoptosis via the intrinsic pathway. Equally, oxidative stress from ID has been shown to promote production of VEGF-A in thyrocytes which is associated with the early phase of tumorigenesis (49). To further assess oxidative stress resulting from IR and from the acute withdrawal of iodine, the expression of NRF2 protein, an oxidative stress biomarker was investigated by western blot. One hour after co-treatment, ID and IR induced NRF2 protein expression in a dose-dependent manner. However, there was no additive effect associated with co-treatment in normal PCCL3 cells. This was in accordance with our preliminary data in which co-treatment was shown to induce ROS production in a dose-dependent manner in FRTL5 and PCCL3 cells. This NRF2 mRNA expression has been demonstrated to be overexpressed in human thyroid cancer cells exposed to oxidative stress (82). Equally, ionizing radiation has been shown to induce overexpression of NRF2 by acting as an antioxidant in Immortilized Mouse Embryonic Fibroblast cells (MEFs) and rats (83) (84). Furthermore, NRF2 transcription has been demonstrated to promote ROS detoxification and enhance proliferation in human pancreatic cancer cell lines (85).

In this study, we observed that radiation-induced oxidative stress in a dose-dependent manner with the highest at 0.5 Gy and 3 Gy irrespective of iodine status which is in accordance with our preliminary results in FRTL5 and PCCL3 cells. We observed an additive effect with ID which is not significant. However, the high standard deviations observed with our western blot cannot be ignored.

Based on this finding, we can conclude that IR and ID induced oxidative stress in a dose-dependent manner though we did not observe a significant additive effect. Hence combined treatment of IR and ID had no additive negative effect as we hypothesized. This result is vital as high expression of NRF2 is an indication of ROS burden. This equally could suggest a carcinogen detoxifying and antioxidant mechanism vital in PCCL3 cytoprotection from the ROS burden. This is in line with a study by Velalopoulou et al., 2015, in which NRF2 was shown to act as cytoprotectant against DNA damage induced by IR in human normal lung cells by acting as a ROS scavenger (86). We further evaluated, ROS (general ROS) production using the CM-H2DCFDA probe following co-treatment of PCCL3 cells. We noted no differential production of ROS at each experimental condition, but this could be attributed to a failure in the experimental setup, as most of our cells died probably due to the wash, mix and read associated with the protocol (**Supplementary Figure 7**). This was contrary to our preliminary results in FRTL5 and PCCL3 cells co-treated with IR and ID induced ROS was relatively successful in measuring ROS production. Due to time constraints, we could not reproduce the results but succeed in evaluating oxidative stress by measuring a known biomarker, NRF2. This oxidative stress is associated with thyroid malignancies like goitre, thyroiditis, thyroid cancer and hyperthyroidism (62). To enable reproducibility of the results in FRTL5 and PCCL3 and validate the oxidative stress we suggest Amplex Red (H_2O_2 and peroxidase activity) or biomarkers of oxidative stress markers reflective of ROS measurement such xanthine oxidase.

ROS production or oxidative stress leads to both genotoxic and non-genotoxic changes in genomic DNA that cause mutations and changes in epigenetic and gene expression respectively. This **DNA damage** from radiation is normally directly or indirectly induced by interaction with water molecules generating hydroxyl radicals. (87). Equally, ID has been shown to be involved in thyroid pathologies via upregulation of antioxidant genes and DNA damage in animal studies (51). To investigate DNA damage from IR and ID, we used the comet assay. Although we observed DNA damage in all doses, none was statistically significant compared to the control with respect to IR, ID or combined treatment. We equally noted that the cells treated with EMS (positive control) did not induce significant DNA damage compared to the controls. To ensure the positive control was effective, we treated normal human blood cells with the same concentration of EMS. Contrary to PCCL3 cells, we observed significant DNA damage in human blood cells compared to all conditions with PCCL3. Taken together, this data suggest that PCCL3 cells are highly resistant to DNA damage directly from IR and ID or indirectly from the generated ROS. We performed the experiments approximately 2 hours after irradiation and had placed the cells immediately on ice after irradiation to prevent DNA damage repair. However, during trypsinization, we had incubated the cells at 37°C for more than 3 minutes as required by the protocol. This could have possibly given the cells enough time to repair any damaged DNA. Equally dose rate is a major factor in radiation-induced cellular response as high dose rate is more damaging. This is demonstrated in a study by Hyun et al., 2016 in which high dose rate (4.68 Gy/min) of 5 Gy induced significant damage in Htori-3 cells compared to a low dose rate (40 mGy/h) of 5 Gy (88). We had use 0.124 Gy/minute which is low dose rate which had possibly permitted the cells to repair any significant DNA damage. Taken together, this data is not in accordance with our preliminary studies on FRTL-5 for which high dose of 3 Gy significantly induced DNA damage. It is equally contrary to study in which normal human thyroid follicular cells experienced significant damage after exposure to doses ranging from 2-12 Gy at a dose rate of

1.5Gy/minute (23). This suggests PCCL3 cells highly resistant to radiation-induced DNA damage compared to other thyroid cells.

Based on this, we performed a RT-qPCR of RAD50 and ATM (two **radiation DNA repair** signaling molecules) 24 hours after co-treatment. Unlike expected, we observed no dose-dependent differential expression in ATM mRNA expression upon co-treatment of cells with IR and ID. On the other hand, we observed a dose-dependent additive effect in RAD50 mRNA expression which was significant at 3 Gy in iodine deficient condition. This is in contrary to results by Guo et al., 2010, in which oxidative stress was shown to activate ATM in 293T cells (human kidney embryonic cells) (89). We equally, noted no activation of TP53 24 hours after co-treatment of cells possibly a confirmation that ATM is not activated (**Supplementary figure 7**). Taken together, this data suggest that the absence of significant DNA damage observed in PCCL3 cells may have resulted from the activation of DNA end-joining pathway which is dependent on the Rad50, Mre11, Nbs1 complex. This is because RAD 50 is required for DSB repair, telomere maintenance hence vital for cell growth and viability. RAD 50 equally acts as a DSBs sensor for ATM and helps ATM to attach to the broken DNA strand (90). However, strangely there is no activation of ATM or p53.

However, to validate the results it is necessary to reduce the handling time for the comet assay. Furthermore, the detection of the gamma H2AX foci with fluorescent microscopy, or performing Poly-ADP-ribose polymerase (PARP) assay will help further investigation of DNA damage. We equally suggest that the genes mentioned above be investigated at earlier time points after irradiation (30 minutes and 1 hour). Moreover, investigating more DNA repair genes such, RAD51 and RAD52 will help validate the results. We equally had used the alkaline version of comet assay, which less sensitive to detect DNA damage compared to the neutral, hence the neutral should be used.

Despite the oxidative stress and/or ROS production generated by IR and ID in PCCL3 cells, these cells are still highly resistant to DNA damage even at high doses. Another possible mechanism to resist DNA damage and apoptosis could be by upregulation of **antioxidant capacity** to counter the oxidative stress. Hence, to investigate the mechanism of radiation resistance in PCCL3 cells, the antioxidant capacity was investigated. This was by measuring the mRNA levels of antioxidant genes like catalase, NQO1 and PRDX5 deprived of iodine and exposed to low, intermediate and high doses of radiation at different time intervals. For PRDX5 at 6 hours, we observed no dose-dependent expression but at 24 hours we observed a dose-dependent expression in iodine sufficient cells which is significant at 3 Gy. However, we did not observe any additive effect with 0.5 Gy and 3 Gy. This is in accordance with results obtained by Weng et al., 2015 in which increased PDRX5 mRNA expression exhibited radioprotection against radiation-induced DNA damage by oxidative stress in human thyroid cells (91). Iodine deficiency alone enhanced PRDX 5 at both 6 and 24 hours compared to iodine sufficient in the absence of irradiation. This is as expected as iodine deficiency has been shown to enhance PRDX 3 and 5 mRNA expression which indicates increase in ROS burden associated with oxidative DNA damage in the thyroid glands of rats and mice (51). Equally, Gerard et al., 2008 demonstrated increased PRDX5 expression under ID condition helping to neutralize ROS associated with goiter and also in basal conditions (92). For catalase mRNA expression, we observed an increased trend in the expression at 6 and 24 hours with respect to radiation. We noted that iodine deficiency-induced a higher expression, however, combined treatment with radiation did not

enhanced expression at 3 Gy. This dose-dependent expression is important as catalase helps in detoxification and scavenging ROS hence, preventing DNA and protein damage that could result from ROS accumulation. This has been shown to be vital in control of cell growth and differentiation apoptosis and immune response. It is a cytoprotective antioxidant enzyme capable of preventing endogenous and exogenous attacks from peroxides (93). Finally, for NQO1, we observed the same trend as with catalase at both 6 and 24 hours as expected. This was expected as it has been demonstrated that IR induces NQO1 preventing radiation-induced aneuploidy which is associated with various human cancers (94). In addition, NQO1 is a target of NRF2 that has been shown to be activated in papillary thyroid carcinoma hence NQO1 dose-dependent expression correlates with NRF2 protein expression. This expression of NQO1 has been demonstrated to be vital in stabilizing and increasing p53 levels, however TP53 was not activated as mentioned earlier (94). Taken together, these results suggest the resistance against DNA damage and apoptosis observed maybe equally due to the high antioxidant capacity of PCCL3 cells as demonstrated by significant expression of PRDX5 and NQO1.

Performing the experiments with a higher number of replicates could increase the possibility of a significant effect. It is equally important to investigate other antioxidant genes such Glutathione, Superoxide Dismutase (SOD) and NQO2 whose dysregulation is associated with Grave's disease and goiter. This is as iodine plays a vital role in inducing cell differentiation and maintaining thyroid tissue homeostasis. Iodine deficiency is associated with decrease organification, hormone secretion and thyroid cell proliferation. Further confirming this expression at protein levels as proteins influence cell phenotype and not mRNA. We experience high standard deviations which should be considered to enhance significance.

We investigated PCCL3 **cell proliferation** during 72 hours following the co-treatment using the real time imaging system called Incucyte. Iodine has been shown to act as an antioxidant and antiproliferation, hence maintains thyroid cell normalcy. As expected, IR and ID significantly enhanced PCCL3 cell proliferation as iodine-deprived cells significantly proliferated better than iodine sufficient cells at all radiation doses as from 40 hours. This is in accordance with the resistance against DNA damage and apoptosis we observed. This is equally in accordance with studies by Boltze et al., 2002 in which they observed rats fed with low iodine diet experienced thyroid hyperproliferation (adenomas) compared to iodine sufficiently fed rats. These same animals developed adenocarcinomas when exposed to high dose IR of 4 Gy (57). In our case of radiation and iodine conditions, the highest proliferation was observed at lower doses (0.05 Gy and 0.1 Gy) while 3 Gy proliferation was slown down to the level of the control. This was expected as PCCL3 cells had exhibited no significant DNA damage and been proven to be radioresistant. Also, ID is known to enhance thyroid cell proliferation independent and or dependent of TSH stimulation (95). We equally observed synergistic effects especially at lower doses as iodine deficient proliferated better after 40 hours in all radiation conditions not supplemented with iodine. However, we notice a decrease in cell proliferation around the 72^{nd} hour compared to the 70^{th} hour as in all conditions, especially at higher doses. This anti-proliferative effect of iodine is usually by the destruction of mitochondrial membrane to initiate apoptosis helping to prevent precancerous transformation. The highest proliferation observed at 0.1 Gy could be explained by hormesis. Taken together, these results suggest the cells resist DNA damage and apoptosis and continue to divide and may bear chromosomal damages. These

chromosomal damages may lead to precancerous transformations. This further confirms the resistance in apoptosis observed. Performing this experiments on human thyroid cells in future experiments will be important.

Based on the proliferation results, we investigated the activation of **proliferation and survival signaling pathways**. We investigated the effects of co-treatment on the activation of JAK/STAT pathway by investigating STAT3 mRNA expression 24 hours post irradiation. As expected, co-treatment induced a trend in STAT3 mRNA expression in a dose-dependent manner while combined treatment had an additive effect on expression at lower doses though non was statistically significant. However, we noted high standard deviations at certain doses which cannot simply be ignored and could explain why we observed no statistical significance between experimental conditions. The dose-dependent trend observed is interesting as this suggest co-treatment may activate the JAK/STAT pathway if the statistical power is increased. This is because STAT3 upregulation has been shown to be associated with thyroid cancer. This is usually by promoting tumor cell proliferation and survival, invasion and immunosuppression (79). Equally, in another study, activated STAT3 was shown to be highly expressed in fibroblast NIH3T3 and Me180 cells exposed to high dose UV (germicidal lamp) and rendered these cells resistant to UV-induced apoptosis (96). To the best of our knowledge there is no study which has investigated the effect of ID on JAK/STAT activation, we observed a high expression of this pathway with ID compared to iodine sufficient conditions. This may suggest the proliferation observed may likely be due to the activation of this pathway. This is important as STAT3 activation is vital in regulation of cell survival, proliferation cyclins and survivin and inflammation associated with cancer. This needs to be investigated further by increasing the number of replicates and altering expression interval after treatment to increase the chance of significance. Furthermore, a Luminex assay should be performed since the JAK/STAT is initiated via binding of cytokines and interleukins such as IFNγ.

PI3K/AKT signaling pathway is vital in cell proliferation and survival, differentiation, migration and apoptosis. Its activation is associated with the development of cancers by inhibiting pro-apoptotic proteins such as Bad, FOXP3a and Bax enabling escape from apoptosis and promoting survival (74). To investigate the activation of this pathway, we investigated AKT1 mRNA expression 24 hours after co-treatment. As expected, we observed a significant dose-dependent expression of mRNA AKT1 expression with respect to radiation. However, post hoc analysis did not reveal specific significant differences between experimental groups. We equally, observed an additive effect with combined treatment however it was not statistically significant and therefore, needs to be investigated further. This could be by increasing the number of replicates and changing the time interval. This is similar to our preliminary results in FRTL-5 and available literature. In one of such studies, Fang et al showed that high dose radiation of 6 Gy activated the PI3K/AKT pathway in GBM cell lines 1 hour after exposure (97). This is also important as activation is associated with activation of other signaling pathways such as NF-KB promoting anti-apoptotic gene upregulation such as Bcl-2 and Bcl-xl and Mcl-1 (72). The higher expression associated with iodine deficiency has not been observed before to the best of our knowledge. This could be that IR activates this pathway by oxidative stress and that further oxidative stress from ID results to the higher activation of this pathway. This data suggests the activation of PI3K/AKT signaling pathway by co-treatment may be responsible for the proliferation

observed. This is vital as activation of this signaling pathway is associated with many types of cancers such as thyroid, glioblastoma, melanoma, pancreatic and lung cancers.

Cyclin D2 is a cell cycle regulator that has been shown to be involved in proliferation via NF-Kβ signaling pathway and is associated with Follicular Thyroid Cancer (FTC). We investigated the activation of CCND2 24 hours after exposure to IR and ID. As anticipated, it exhibited the same dose-dependent expression as AKT1, which was significant at 3 Gy in both iodine deficient and iodine sufficient conditions. This is a significant result as cyclin D2 is vital in cell cycle regulation, differentiation and malignant control. This adds to CCND1 which we had observed in our preliminary data. CCND2 is a key regulator of G1 cell cycle progression and proliferation is associated with oncogenesis when overexpressed (98). This data suggest an unusual deregulated G1-S checkpoint as a possible decisive activity for PCCL3 cells. We, however, did not find any study in the literature which investigates the effect of IR or ID on thyroid cancer. It will be interesting to reproduce this observation at the level of protein expression.

We evaluated apoptosis from the co-treated cells with IR and ID using the caspase-3/7 and Annexin V multi-kinetic assay using the IcuCyte. Unsurprisingly, we observed significant cell death at 0.5 Gy and 3 Gy in both iodine deficient and iodine sufficient conditions after 48 hours. However, co-treatment failed to induce significant cell death at low doses. This confirmed similar preliminary results observed in FRTL-5 cells from rat origin in our initial results. 72 hours post co-treatment all the irradiated cells experienced significant cell death which was highest at 3 Gy in both iodine conditions. The apoptotic cell death after 72 hours could also probably be due to a shortage of nutrients and space. Despite these observations, we observed no synergistic effect and majority of the cells continued to divide which is contrary to our hypothesis. The resistant we observed at low dose was expected as thyroid cells are considered to be very resistant to acute effects of IR. This supports our gene expression analyses. These similar results have been observed in thyroid cells (FRTL-5) exposed to UV-radiation (99). Equally, radiation from I^{131} has been shown to initiate apoptosis in human epithelial thyroid cells (100). However, our caspase staining failed so we could not analyze the data obtained from the images. Hence apoptosis via caspase-3 or 7 could not be evaluated. It will be interesting to perform the experiment with a caspase-3/7 reagent to investigate the resistant observed at low doses after 48 hours. Iodine deficiency has been shown to increase delayed apoptosis in the rat (101), we, therefore, had expected a higher induction of apoptosis in co-treated cells. Unfortunately, we observed no significant differences between iodine supplemented and iodine deficient cells. This data suggest that radiation and ID induced apoptosis in a long-term manner and not acute as we observed no significant apoptosis at 24 hours and only exhibited apoptosis at intermediate and high doses after 48 hours. Equally, after 72 hours all doses show significant cell death supporting the possibility of a time factor. Despite the cells undergoing radiation induced apoptosis, this is not enough to stop cell division in conditions deprived of iodine. Based on this data, it seems the cells resist apoptosis from low dose radiation and ID but could not withstand the high dose radiation especially when deprived of iodine.

To investigate this radioresistance observed in PCCL3 cells with regards to apoptosis and DNA damage. We investigated **anti-apoptotic** mRNA expression of Bcl-2 and Mcl-1 24 hours post iodine

deprivation and irradiation. Bcl-2 dysregulation is associated with many malignancies such as breast, melanoma, lung and leukemia. Overexpression of Bcl-2 is known to confer resistance to radiation-induced apoptosis (102). As anticipated, we observed a dose-dependent increase in expression of Bcl-2 mRNA, which was significant at 3 Gy compared to the control in both iodine deficient and iodine sufficient conditions. Equally, 3 Gy was significant compared to 0.05 Gy and 0.1Gy in both iodine conditions. This result was expected as it suggests the cells resisted apoptosis and DNA damage especially at low doses and continued to proliferate despite some cell death. Similar results were obtained in studies by Chorna et al., 2005 in which breast cancer cells, (MCF-7) cells irradiated with low dose X-ray exhibited increased DNA repair and resistance to apoptosis via increased expression of Bcl-2 (103). GS Choudary et al., 2015 had similar results in Diffuse Large B-Cell Lymphoma (DLBCL) in which the cells resisted apoptosis induced by venetoclax by overexpression of Bcl-2 (104). Our finding suggests the modulation of the pro-survival gene, Bcl-2 may be responsible for resistance to apoptosis observed especially at an early time-point in low doses in PCCL3. However, it will be interesting to investigate this at the protein level either by western blot or ELISA. It will also be important to investigate the expression of Bax, Bcl-xl Bak and Bim which are inhibited by Bcl-2 to render the cells resistant to radiation-induced apoptosis in thyroid carcinoma cells (105).

Mcl-1 is an anti-apoptotic protein which promotes cell survival by sequestration of pro-apoptotic Bak, Bad and Bim and is usually associated with resistance to radiation-induced apoptosis. Mcl-1 upregulation has been observed to enhance cell survival in breast and non-small cell lung cancer melanoma (106). As expected, we observed a dose-dependent expression of Mcl-1 mRNA expression 24 hours following co-treatment with the highest expression at 3 Gy in both iodine sufficient and iodine deficient conditions. However, post hoc testing did not reveal specific differences between experimental groups. No additive effect was observed at 0 Gy, 0.5 Gy and 3 Gy. Hans et al., 2005 observed similar results in 518A2 melanoma cells in which all melanoma cell lines analyzed highly expressed Mcl-1 mRNA at 24, 48 and 72 hours following irradiation with high dose radiation of 4 Gy (107). This finding suggests that Mcl-1 together with Bcl-2 may play a key role in radioresistance of PCCL3 cells. It will be interesting, nonetheless, to perform the experiments with more replicates and at different time intervals. This will probably help to increase the significance. It will equally be important to investigate the expression at the protein level as protein influence cell behavior and not mRNA.

Finally, we investigated the effects of the co-treatment on CLIP2, a radiation-dependent thyroid cancer biomarker (**radiation expensive element**). This is because CLIP2 has been reportedly expressed at the mRNA and protein levels in radiation-induced thyroid cancer as seen in post-Chernobyl samples (108). The expression of CLIP2 was investigated at 24 and 72 hours following co-treatment. At 24 hours, we observed a dose-dependent increase in CLIP2 expression though this is not significant. Unexpectedly, we observed no differential expression of CLIP2 at 72hours regardless of dose or iodine status. At 24 hours, the trend in expression is similar to that obtained in post-Chernobyl samples in which a dose-dependent expression of CLIP2 mRNA was observed with high doses (3-6 Gy),(109) while contrary at 72 hours in which we observed no trend. The observation at 24 hours is important as CLIP2 has been suggested to be a key player in thyroid carcinogenesis through genome instability, pro-apoptotic and signaling pathways like the MAPK (110). It will be

interesting to further investigate CLIP2 at 24 hours with a higher number of replicates to increase the possibility of significance and also at the protein level.

We encountered some limitations during this project which include but not limited to the cell type used. PCCL3 is a continuous cell line which continues to evolve in culture and may lose some of their thyroid characteristics and possibly may not give an accurate reflection of the thyroid. It is equally possible that this cell line may not be the ideal cell line for this experiments even if they are commonly used in iodine deficiency experiments (49). Human epithelial cells will be ideal, unfortunately, they are limited in passage number (maximum of 9) which makes it difficult to be used for experiments requiring a large number of cells. Moreover, the only commercially available normal human thyroid cells (H6040) were discontinued. It is hard to obtain an ideal cell line for this experiments involving the co-treatment of IR and ID. Equally, due to time constraint, we could use a known cell line that expressed our genes of interest in our qPCR analyses. Our use of NRF-2 as a biomarker of oxidative stress was also a limitation as it is the measure of antioxidant capacity and not direct ROS. Our gene expression profiling was performed at the level of mRNA, whose abundance is less conserved than protein and hence might not influence cell behavior (111). Furthermore, our comet assay focused on DSBs and SSBs, which are the most common. However, there other DNA damages that could be associated with exposure to radiation such as interstrand crosslink . It will equally be necessary to investigate micronucleus formation indicative of chromatid and chromosome damage.

We had hypothesized at the beginning of this project that low dose radiation and ID have an additive negative effect on thyrocytes via induction of damaging levels of oxidative stress, potentially leading to activation of precancerous pathways. These results seemed supportive of this hypothesis. Nevertheless, there is need to further research in detail to understand the effects of low doses ionizing radiation and iodine deficiency. This is as co-treatment of cells with ID and IR induced significant oxidative stress at 0.5 Gy and 3 Gy 1 hour after treatment. However, this oxidative stress could not induce significant DNA damage even at intermediate and high doses irrespective of iodine status. RAD50, involved in DNA damage repair had a synergistic effect on 3Gy suggesting it could be responsible for repair. This suggests that PCCL3 are highly resistant to the double stress of IR and ID. When we examined the proliferation of cells, we observed a synergistic effect on iodine deficient cells especially at low dose 0.05 Gy and 0.1 Gy boosted cell proliferation. Furthermore, we noticed significant cell death at 48 hours at 3 Gy and at all doses after 72 hours. This indicates that PCCL3 cells not only resisted radiation-induced DNA damage but apoptosis at low and intermediate doses but succumbed at higher doses. At 72 hours, all doses experienced apoptosis compared to the control, and this could be as a result of a shortage in nutrients and space. This means that PCCL3 cells exhibited a high resistance profile to apoptosis as confirmed by a dose-dependent increase in the expression of anti-apoptotic genes, Bcl-2 and Mcl-1 24 hours after co-treatment. Furthermore, we observed a dose-dependent trend in the activation of proliferation and survival signaling pathways, which suggests oxidative stress is able to activate these pathways. This suggests the activation of these pathways that are essential among others in precancerous transformations. Moreover, CCND2 is activated in a dose-dependent manner and significant at 3Gy irrespective of iodine status. This shows the overexpression of an additional factor essential for precancerous transformation. We equally observed dose-dependent expression of antioxidant genes NQO1, PRDX5 and NRF2, which suggest these genes might be responsible for the resistance of PCCL3 cells to

oxidative stress. Finally, CLIP2, a biomarker of radiation-induced thyroid cancer was not significantly upregulated possibly because the time frame was too early. Furthermore, these results seem to suggest that despite the apoptosis observed this is not sufficient to stop cell division. Based on this, we can conclude that PCCL3 cells are highly resistant to apoptosis and DNA damage induced by oxidative stress from IR and ID. Further experiments are needed to validate ithe survival mechanisms or apoptosis annd DNA damage resistance mechanisms against low doses of radiation under iodine deficiency condition.

With regards to the future perspective, we suggest investigating the changes in gene expression profiling at different time intervals while increasing the number of replicates. Furthermore, we suggest the investigation of the protein abundance of those genes which showed significant activation. We equally suggest investigating further survival pathways such as β-catenin pathway, MAPK pathway and NOTCH pathway. Finally, human thyroid cell lines, in vivo models and chronic/or fluctuating iodine deficiency should be used to further investigate these results if they are to be translated to the human situation.

5 REFERENCES

1. Melmed S, Polonsky KS, Larsen PR, Kronenberg HM. Williams textbook of endocrinology: Elsevier Health Sciences; 2015.
2. Ventura-Holman T, Mamoon A, Maher JF, Subauste JS. Thyroid hormone responsive genes in the murine hepatocyte cell line AML 12. Gene. 2007;396(2):332-7.
3. Zimmermann MB, editor The role of iodine in human growth and development. Seminars in cell & developmental biology; 2011: Elsevier.
4. Pellegriti G, Frasca F, Regalbuto C, Squatrito S, Vigneri R. Worldwide increasing incidence of thyroid cancer: update on epidemiology and risk factors. Journal of cancer epidemiology. 2013;2013.
5. Van den Bruel A, Maes A, De Potter T, Mortelmans L, Drijkoningen M, Van Damme B, et al. Clinical relevance of thyroid fluorodeoxyglucose-whole body positron emission tomography incidentaloma. The Journal of Clinical Endocrinology & Metabolism. 2002;87(4):1517-20.
6. Kitahara CM, Sosa JA. The changing incidence of thyroid cancer. Nature Reviews Endocrinology. 2016.
7. Vecchia C, Malvezzi M, Bosetti C, Garavello W, Bertuccio P, Levi F, et al. Thyroid cancer mortality and incidence: a global overview. International Journal of Cancer. 2015;136(9):2187-95.
8. Manole D, Schildknecht B, Gosnell B, Adams E, Derwahl M. Estrogen Promotes Growth of Human Thyroid Tumor Cells by Different Molecular Mechanisms 1. The Journal of Clinical Endocrinology & Metabolism. 2001;86(3):1072-7.
9. Von Behren J, Lipsett M, Horn-Ross PL, Delfino RJ, Gilliland F, McConnell R, et al. Obesity, waist size and prevalence of current asthma in the California Teachers Study cohort. Thorax. 2009;64(10):889-93.
10. Katoh H, Yamashita K, Enomoto T, Watanabe M. Classification and general considerations of thyroid cancer. Ann Clin Pathol. 2015;3(1):1045.
11. Trovisco V, Soares P, Preto A, de Castro IV, Lima J, Castro P, et al. Type and prevalence of BRAF mutations are closely associated with papillary thyroid carcinoma histotype and patients' age but not with tumour aggressiveness. Virchows Arch. 2005;446(6):589-95.
12. Gertz RJ, Nikiforov Y, Rehrauer W, McDaniel L, Lloyd RV. Mutation in BRAF and Other Members of the MAPK Pathway in Papillary Thyroid Carcinoma in the Pediatric Population. Arch Pathol Lab Med. 2016;140(2):134-9.
13. Xing M. Recent advances in molecular biology of thyroid cancer and their clinical implications. Otolaryngol Clin North Am. 2008;41(6):1135-46, ix.
14. Buffet C, Groussin L. Molecular perspectives in differentiated thyroid cancer. Ann Endocrinol (Paris). 2015;76(1 Suppl 1):1S8-15.
15. Galofré JC, Calleja A, Panizo A, Salvador J. [Molecular biology of follicular thyroid carcinoma (II). Clinical applications]. Rev Med Univ Navarra. 2003;47(2):23-9.
16. Are C, Shaha AR. Anaplastic thyroid carcinoma: biology, pathogenesis, prognostic factors, and treatment approaches. Ann Surg Oncol. 2006;13(4):453-64.
17. Xing M. Molecular pathogenesis and mechanisms of thyroid cancer. Nat Rev Cancer. 2013;13(3):184-99.
18. Wagner SM, Zhu S, Nicolescu AC, Mulligan LM. Molecular mechanisms of RET receptor-mediated oncogenesis in multiple endocrine neoplasia 2. Clinics (Sao Paulo). 2012;67 Suppl 1:77-84.
19. Cousins C. ICRP and Radiological Protection in Medicine. Radiat Prot Dosimetry. 2016.
20. Sinnott B, Ron E, Schneider AB. Exposing the thyroid to radiation: a review of its current extent, risks, and implications. Endocr Rev. 2010;31(5):756-73.
21. Vanmarcke H. UNsCEAR 2000: sources of ionizing radiation. Ann Ass Belge de Radioprot. 2002;27:41-65.
22. Brenner DJ, Doll R, Goodhead DT, Hall EJ, Land CE, Little JB, et al. Cancer risks attributable to low doses of ionizing radiation: assessing what we really know. Proceedings of the National Academy of Sciences. 2003;100(24):13761-6.

23. Green LM, Murray DK, Tran DT, Bant AM, Kazarians G, Moyers MF, et al. Response of thyroid follicular cells to gamma irradiation compared to proton irradiation. I. Initial characterization of DNA damage, micronucleus formation, apoptosis, cell survival, and cell cycle phase redistribution. Radiation research. 2001;155(1):32-42.
24. Szumiel I. Ionizing radiation-induced oxidative stress, epigenetic changes and genomic instability: the pivotal role of mitochondria. International journal of radiation biology. 2015;91(1):1-12.
25. Astakhova LN, Anspaugh LR, Beebe GW, Bouville A, Drozdovitch VV, Garber V, et al. Chernobyl-related thyroid cancer in children of Belarus: a case-control study. Radiation research. 1998;150(3):349-56.
26. Ron E, Lubin JH, Shore RE, Mabuchi K, Modan B, Pottern LM, et al. Thyroid cancer after exposure to external radiation: a pooled analysis of seven studies. Radiation research. 1995;141(3):259-77.
27. Cardis E, Krewski D, Boniol M, Drozdovitch V, Darby SC, Gilbert ES, et al. Estimates of the cancer burden in Europe from radioactive fallout from the Chernobyl accident. International Journal of Cancer. 2006;119(6):1224-35.
28. Cardis E, Hatch M. The Chernobyl accident—an epidemiological perspective. Clinical Oncology. 2011;23(4):251-60.
29. Tronko MD, Howe GR, Bogdanova TI, Bouville AC, Epstein OV, Brill AB, et al. A cohort study of thyroid cancer and other thyroid diseases after the Chornobyl accident: thyroid cancer in Ukraine detected during first screening. Journal of the National Cancer Institute. 2006;98(13):897-903.
30. Gilbert ES, Huang L, Bouville A, Berg CD, Ron E. Thyroid cancer rates and 131I doses from Nevada atmospheric nuclear bomb tests: an update. Radiation research. 2010;173(5):659-64.
31. Yamashita S, Suzuki S. Risk of thyroid cancer after the Fukushima nuclear power plant accident. Respiratory investigation. 2013;51(3):128-33.
32. De Vathaire F, Drozdovitch V, Brindel P, Rachedi F, Boissin JL, Sebbag J, et al. Thyroid cancer following nuclear tests in French Polynesia. British journal of cancer. 2010;103(7):1115-21.
33. Bollaerts K, Sonck M, Simons K, Fierens S, Poffijn A, Van Bladel L, et al. Thyroid cancer incidence around the Belgian nuclear sites: Surrogate exposure modelling. Cancer epidemiology. 2015;39(1):48-54.
34. Wartofsky L. Increasing world incidence of thyroid cancer: increased detection or higher radiation exposure. Hormones (Athens). 2010;9(2):103-8.
35. Hall EJ. Radiation biology for pediatric radiologists. Pediatric radiology. 2009;39(1):57-64.
36. Chodick G, Ronckers CM, Shalev V, Ron E. Excess lifetime cancer mortality risk attributable to radiation exposure from computed tomography examinations in children. IMAJ-RAMAT GAN-. 2007;9(8):584.
37. Sadetzki S, Chetrit A, Lubina A, Stovall M, Novikov I. Risk of Thyroid Cancer after Childhood Exposure to Ionizing Radiation for Tinea Capitis 1. The Journal of Clinical Endocrinology & Metabolism. 2006;91(12):4798-804.
38. Schneider AB, Ron E, Lubin J, Stovall M, Gierlowski TC. Dose-response relationships for radiation-induced thyroid cancer and thyroid nodules: evidence for the prolonged effects of radiation on the thyroid. The Journal of Clinical Endocrinology & Metabolism. 1993;77(2):362-9.
39. Neta G, Rajaraman P, de Gonzalez AB, Doody MM, Alexander BH, Preston D, et al. A prospective study of medical diagnostic radiography and risk of thyroid cancer. American journal of epidemiology. 2013;177(8):800-9.
40. Dawson P, Punwani S. The thyroid dose burden in medical imaging: a re-examination. European journal of radiology. 2009;69(1):74-9.
41. Inskip PD, Ekbom A, Galanti MR, Grimelius L, Boice JD. Medical diagnostic x rays and thyroid cancer. Journal of the National Cancer Institute. 1995;87(21):1613-21.
42. Schonfeld SJ, Lee C, de Gonzalez AB. Medical exposure to radiation and thyroid cancer. Clinical Oncology. 2011;23(4):244-50.

43. Taurog A. Hormone synthesis: thyroid iodine metabolism. Werner & Ingbar's The Thyroid: a fundamental and clinical text 8th ed Philadelphia: Lippincott, Williams & Wilkins. 2000:61-85.
44. Truong T, Baron-Dubourdieu D, Rougier Y, Guénel P. Role of dietary iodine and cruciferous vegetables in thyroid cancer: a countrywide case–control study in New Caledonia. Cancer Causes & Control. 2010;21(8):1183-92.
45. Cléro É, Doyon F, Chungue V, Rachédi F, Boissin J-L, Sebbag J, et al. Dietary patterns, goitrogenic food, and thyroid cancer: a case-control study in French Polynesia. Nutrition and cancer. 2012;64(7):929-36.
46. Kim HJ, Kim NK, Park HK, Byun DW, Suh K, Yoo MH, et al. Strong association of relatively low and extremely excessive iodine intakes with thyroid cancer in an iodine-replete area. European journal of nutrition. 2016:1-7.
47. Roger PP, Dumont JE. Factors controlling proliferation and differentiation of canine thyroid cells cultured in reduced serum conditions: effects of thyrotropin, cyclic AMP and growth factors. Molecular and cellular endocrinology. 1984;36(1):79-93.
48. Knobel M, Medeiros-Neto G. Relevance of iodine intake as a reputed predisposing factor for thyroid cancer. Arquivos Brasileiros de Endocrinologia & Metabologia. 2007;51(5):701-12.
49. Gérard A-C, Poncin S, Audinot J-N, Denef J-F, Colin IM. Iodide deficiency-induced angiogenic stimulus in the thyroid occurs via HIF-and ROS-dependent VEGF-A secretion from thyrocytes. American Journal of Physiology-Endocrinology and Metabolism. 2009;296(6):E1414-E22.
50. Craps J, Wilvers C, Joris V, De Jongh B, Vanderstraeten J, Lobysheva I, et al. Involvement of nitric oxide in iodine deficiency-induced microvascular remodeling in the thyroid gland: role of nitric oxide synthase 3 and ryanodine receptors. Endocrinology. 2014;156(2):707-20.
51. Maier J, Van Steeg H, Van Oostrom C, Paschke R, Weiss RE, Krohn K. Iodine deficiency activates antioxidant genes and causes DNA damage in the thyroid gland of rats and mice. Biochimica et Biophysica Acta (BBA)-Molecular Cell Research. 2007;1773(6):990-9.
52. Krohn K, Maier J, Paschke R. Mechanisms of disease: hydrogen peroxide, DNA damage and mutagenesis in the development of thyroid tumors. Nature clinical practice Endocrinology & metabolism. 2007;3(10):713-20.
53. Aceves C, Anguiano B, Delgado G. The extrathyronine actions of iodine as antioxidant, apoptotic, and differentiation factor in various tissues. Thyroid. 2013;23(8):938-46.
54. Gembicki M, Stozharov AN, Arinchin AN, Moschik KV, Petrenko S, Khmara IM, et al. Iodine deficiency in Belarusian children as a possible factor stimulating the irradiation of the thyroid gland during the Chernobyl catastrophe. Environmental health perspectives. 1997;105(Suppl 6):1487.
55. Nikiforov YE, Rowland JM, Bove KE, Monforte-Munoz H, Fagin JA. Distinct pattern of ret oncogene rearrangements in morphological variants of radiation-induced and sporadic thyroid papillary carcinomas in children. Cancer Research. 1997;57(9):1690-4.
56. Shakhtarin VV, Tsyb AF, Stepanenko VF, Orlov MY, Kopecky KJ, Davis S. Iodine deficiency, radiation dose, and the risk of thyroid cancer among children and adolescents in the Bryansk region of Russia following the Chernobyl power station accident. International journal of epidemiology. 2003;32(4):584-91.
57. Boltze C, Brabant G, Dralle H, Gerlach R, Roessner A, Hoang-Vu C. Radiation-induced thyroid carcinogenesis as a function of time and dietary iodine supply: an in vivo model of tumorigenesis in the rat. Endocrinology. 2002;143(7):2584-92.
58. Zimmermann MB, Galetti V. Iodine intake as a risk factor for thyroid cancer: a comprehensive review of animal and human studies. Thyroid research. 2015;8(1):1.
59. Shi X, Zhang Y, Zheng J, Pan J. Reactive oxygen species in cancer stem cells. Antioxidants & redox signaling. 2012;16(11):1215-28.
60. Huang W, Xing W, Li D, Liu Y. Microcystin-RR induced apoptosis in tobacco BY-2 suspension cells is mediated by reactive oxygen species and mitochondrial permeability transition pore status. Toxicology in Vitro. 2008;22(2):328-37.
61. Pacifico F, Leonardi A. Role of NF-κB in thyroid cancer. Molecular and cellular endocrinology. 2010;321(1):29-35.

62. Xing M. Oxidative stress: a new risk factor for thyroid cancer. Endocrine-related cancer. 2012;19(1):C7-C11.
63. Wang D, Feng J-F, Zeng P, Yang Y-H, Luo J, Yang Y-W. Total oxidant/antioxidant status in sera of patients with thyroid cancers. Endocrine-related cancer. 2011;18(6):773-82.
64. Ameziane-El-Hassani R, Talbot M, Dos Santos MCdS, Al Ghuzlan A, Hartl D, Bidart J-M, et al. NADPH oxidase DUOX1 promotes long-term persistence of oxidative stress after an exposure to irradiation. Proceedings of the National Academy of Sciences. 2015;112(16):5051-6.
65. Borrego-Soto G, Ortiz-López R, Rojas-Martínez A. Ionizing radiation-induced DNA injury and damage detection in patients with breast cancer. Genetics and molecular biology. 2015;38(4):420-32.
66. Langerak P, Russell P. Regulatory networks integrating cell cycle control with DNA damage checkpoints and double-strand break repair. Phil Trans R Soc B. 2011;366(1584):3562-71.
67. Jeggo P, Löbrich M. Radiation-induced DNA damage responses. Radiation protection dosimetry. 2006;122(1-4):124-7.
68. Palanisamy N, Ateeq B, Kalyana-Sundaram S, Pflueger D, Ramnarayanan K, Shankar S, et al. Rearrangements of the RAF kinase pathway in prostate cancer, gastric cancer and melanoma. Nature medicine. 2010;16(7):793-8.
69. Nucera C, Porrello A, Antonello ZA, Mekel M, Nehs MA, Giordano TJ, et al. B-RafV600E and thrombospondin-1 promote thyroid cancer progression. Proceedings of the National Academy of Sciences. 2010;107(23):10649-54.
70. Dent P, Yacoub A, Fisher PB, Hagan MP, Grant S. MAPK pathways in radiation responses. Oncogene. 2003;22(37):5885-96.
71. Robbins HL, Hague A. The PI3K/Akt Pathway in Tumors of Endocrine Tissues. Frontiers in endocrinology. 2015;6.
72. Zhan M, Han ZC. Phosphatidylinositide 3-kinase AKT in radiation responses. 2004.
73. Guigon CJ, Zhao L, Willingham MC, Cheng SY. PTEN deficiency accelerates tumour progression in a mouse model of thyroid cancer. Oncogene. 2009;28(4):509-17.
74. Liu B, Kuang A. [Genetic alterations in MAPK and PI3K/Akt signaling pathways and the generation, progression, diagnosis and therapy of thyroid cancer]. Sheng wu yi xue gong cheng xue za zhi= Journal of biomedical engineering= Shengwu yixue gongchengxue zazhi. 2012;29(6):1221-5.
75. DiDonato JA, Mercurio F, Karin M. NF-κB and the link between inflammation and cancer. Immunological reviews. 2012;246(1):379-400.
76. Ahmed KM, Li JJ. NF-κB-mediated adaptive resistance to ionizing radiation. Free Radical Biology and Medicine. 2008;44(1):1-13.
77. Hoesel B, Schmid JA. The complexity of NF-κB signaling in inflammation and cancer. Molecular cancer. 2013;12(1):1.
78. Dreesen O, Brivanlou AH. Signaling pathways in cancer and embryonic stem cells. Stem cell reviews. 2007;3(1):7-17.
79. Sosonkina N, Starenki D, Park J-I. The role of STAT3 in thyroid cancer. Cancers. 2014;6(1):526-44.
80. Couto JP, Daly L, Almeida A, Knauf JA, Fagin JA, Sobrinho-Simões M, et al. STAT3 negatively regulates thyroid tumorigenesis. Proceedings of the National Academy of Sciences. 2012;109(35):E2361-E70.
81. Singh S, Vrishni S, Singh BK, Rahman I, Kakkar P. Nrf2-ARE stress response mechanism: a control point in oxidative stress-mediated dysfunctions and chronic inflammatory diseases. Free radical research. 2010;44(11):1267-88.
82. Cha H-Y, Lee B-S, Chang JW, Park JK, Han JH, Kim Y-S, et al. Downregulation of Nrf2 by the combination of TRAIL and Valproic acid induces apoptotic cell death of TRAIL-resistant papillary thyroid cancer cells via suppression of Bcl-xL. Cancer letters. 2016;372(1):65-74.
83. Frijhoff J, Winyard PG, Zarkovic N, Davies SS, Stocker R, Cheng D, et al. Clinical relevance of biomarkers of oxidative stress. Antioxidants & redox signaling. 2015;23(14):1144-70.
84. McDonald JT, Kim K, Norris AJ, Vlashi E, Phillips TM, Lagadec C, et al. Ionizing radiation activates the Nrf2 antioxidant response. Cancer research. 2010;70(21):8886-95.

85. DeNicola GM, Chen P-H, Mullarky E, Sudderth JA, Hu Z, Wu D, et al. NRF2 regulates serine biosynthesis in non-small cell lung cancer. Nature genetics. 2015;47(12):1475.
86. Velalopoulou A, Tyagi S, Pietrofesa RA, Arguiri E, Christofidou-Solomidou M. The flaxseed-derived lignan phenolic secoisolariciresinol diglucoside (SDG) protects non-malignant lung cells from radiation damage. International journal of molecular sciences. 2015;17(1):7.
87. Wu Q, Ni X. ROS-mediated DNA methylation pattern alterations in carcinogenesis. Current drug targets. 2015;16(1):13-9.
88. Bang HS, Choi MH, Kim CS, Choi SJ. Gene expression profiling in undifferentiated thyroid carcinoma induced by high-dose radiation. Journal of radiation research. 2016:rrw002.
89. Guo Z, Kozlov S, Lavin MF, Person MD, Paull TT. ATM activation by oxidative stress. Science. 2010;330(6003):517-21.
90. Lee J-H, Mand MR, Deshpande RA, Kinoshita E, Yang S-H, Wyman C, et al. Ataxia telangiectasia-mutated (ATM) kinase activity is regulated by ATP-driven conformational changes in the Mre11/Rad50/Nbs1 (MRN) complex. Journal of Biological Chemistry. 2013;288(18):12840-51.
91. Walbrecq G, Wang B, Becker S, Hannotiau A, Fransen M, Knoops B. Antioxidant cytoprotection by peroxisomal peroxiredoxin-5. Free Radical Biology and Medicine. 2015;84:215-26.
92. Poncin S, Gérard A-C, Boucquey M, Senou M, Calderon PB, Knoops B, et al. Oxidative stress in the thyroid gland: from harmlessness to hazard depending on the iodine content. Endocrinology. 2008;149(1):424-33.
93. Ameziane-El-Hassani R, Boufraqech M, Lagente-Chevallier O, Weyemi U, Talbot M, Métivier D, et al. Role of H2O2 in RET/PTC1 chromosomal rearrangement produced by ionizing radiation in human thyroid cells. Cancer research. 2010;70(10):4123-32.
94. Park M-T, Oh E-T, Song M-J, Lee H, Choi EK, Park HJ. NQO1 prevents radiation-induced aneuploidy by interacting with Aurora-A. Carcinogenesis. 2013:bgt225.
95. Gérard A-C, Poncin S, Caetano B, Sonveaux P, Audinot J-N, Feron O, et al. Iodine deficiency induces a thyroid stimulating hormone-independent early phase of microvascular reshaping in the thyroid. The American journal of pathology. 2008;172(3):748-60.
96. Shen Y, Devgan G, Darnell JE, Bromberg JF. Constitutively activated Stat3 protects fibroblasts from serum withdrawal and UV-induced apoptosis and antagonizes the proapoptotic effects of activated Stat1. Proceedings of the National Academy of Sciences. 2001;98(4):1543-8.
97. Li H-F, Kim J-S, Waldman T. Radiation-induced Akt activation modulates radioresistance in human glioblastoma cells. Radiation oncology. 2009;4(1):43.
98. Evron E, Umbricht CB, Korz D, Raman V, Loeb DM, Niranjan B, et al. Loss of cyclin D2 expression in the majority of breast cancers is associated with promoter hypermethylation. Cancer research. 2001;61(6):2782-7.
99. Del Terra E, Francesconi A, Donnini D, Curcio F, Ambesi-Impiombato FS. Thyrotropin effects on ultraviolet radiation-dependent apoptosis in FRTL-5 cells. Thyroid. 2003;13(8):747-53.
100. Russo E, Guerra A, Marotta V, Faggiano A, Colao A, Del Vecchio S, et al. Radioiodide induces apoptosis in human thyroid tissue in culture. Endocrine. 2013;44(3):729-34.
101. Dong J, Wang Y, Wang Y, Wei W, Min H, Song B, et al. Iodine deficiency increases apoptosis and decreases synaptotagmin-1 and PSD-95 in rat hippocampus. Nutritional neuroscience. 2013;16(3):135-41.
102. P. Hoyes WBCCSPJHHK. Effect of bcl-2 deficiency on the radiation response of clonogenic cells in small and large intestine, bone marrow and testis. International journal of radiation biology. 2000;76(11):1435-42.
103. Chorna IV, Datsyuk LO, Stoika RS. Expression of Bax, Bad and Bcl-2 proteins under x-radiation effect towards human breast carcinoma MCF-7 cells and their doxorubicin-resistant derivatives. Exp Oncol. 2005;27(3):196-201.
104. Choudhary GS, Al-Harbi S, Mazumder S, Hill BT, Smith MR, Bodo J, et al. MCL-1 and BCL-xL-dependent resistance to the BCL-2 inhibitor ABT-199 can be overcome by preventing PI3K/AKT/mTOR activation in lymphoid malignancies. Cell death & disease. 2015;6(1):e1593.

105. Mitsiades CS, Hayden P, Kotoula V, McMillin DW, McMullan C, Negri J, et al. Bcl-2 overexpression in thyroid carcinoma cells increases sensitivity to Bcl-2 homology 3 domain inhibition. The Journal of Clinical Endocrinology & Metabolism. 2007;92(12):4845-52.
106. Bruncko M, Wang L, Sheppard GS, Phillips DC, Tahir SK, Xue J, et al. Structure-guided design of a series of MCL-1 inhibitors with high affinity and selectivity. Journal of medicinal chemistry. 2015;58(5):2180-94.
107. Skvara H, Thallinger C, Wacheck V, Monia BP, Pehamberger H, Jansen B, et al. Mcl-1 blocks radiation-induced apoptosis and inhibits clonogenic cell death. Anticancer research. 2005;25(4):2697-703.
108. Thomas G, Unger K, Krznaric M, Galpine A, Bethel J, Tomlinson C, et al. The chernobyl tissue bank—a repository for biomaterial and data used in integrative and systems biology modeling the human response to radiation. Genes. 2012;3(2):278-90.
109. Selmansberger M, Kaiser JC, Hess J, Güthlin D, Likhtarev I, Shpak V, et al. Dose-dependent expression of CLIP2 in post-Chernobyl papillary thyroid carcinomas. Carcinogenesis. 2015;36(7):748-56.
110. Philchenkov AA, Balcer-Kubiczek EK. Molecular markers of apoptosis in cancer patients exposed to ionizing radiation: the post-Chornobyl view. Experimental Oncology. 2016;38(4):224-37.
111. Laurent JM, Vogel C, Kwon T, Craig SA, Boutz DR, Huse HK, et al. Protein abundances are more conserved than mRNA abundances across diverse taxa. Proteomics. 2010;10(23):4209-12.

SUPPLEMENTARY DATA

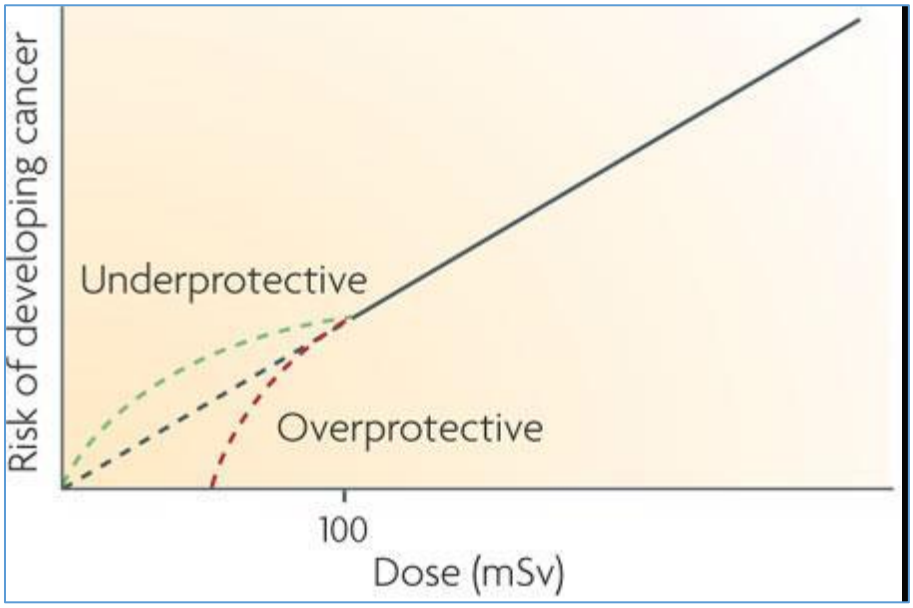

Supplementary Figure 1: The relation between low dose ionizing radiation and the risk of cancer. Below the known threshold of 100mSv (solid blackline) the biological effects are not exactly clear. So a linear non-threshold model is often used to estimate the risk of cancer below the 100mSv threshold (broken blackline) (14).

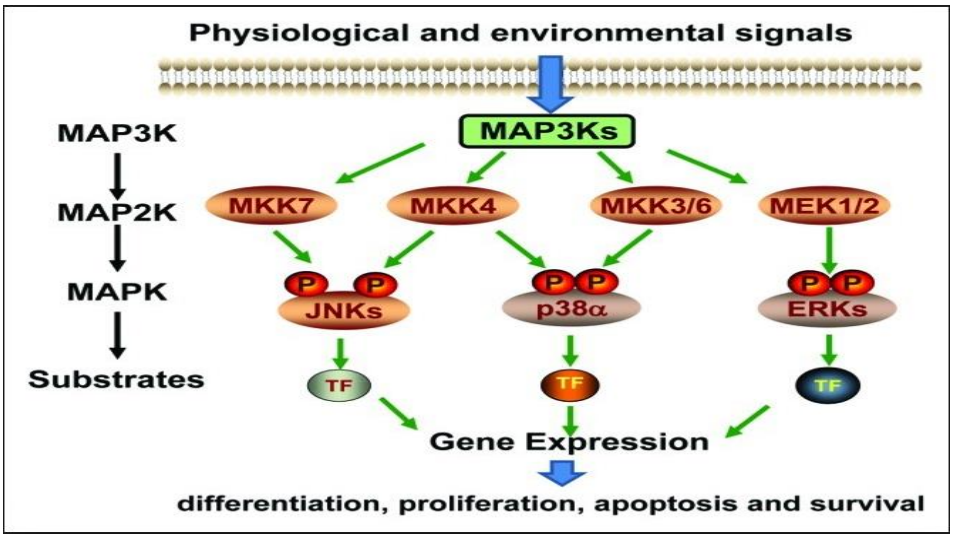

Supplementary figure 2: **Radiation activation of the MAPK signaling pathway**

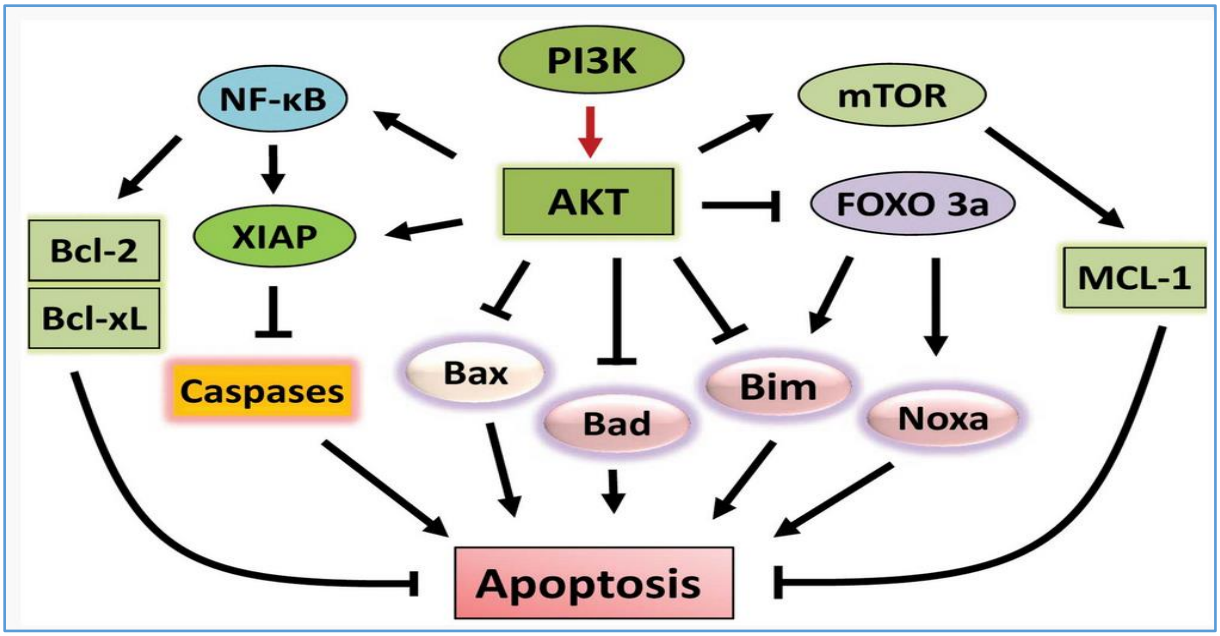

Supplementary figure 3: Radiation activation of PI3K/AKT pathway promotes cell survival. Phosphorylation of AKT leads to transcription of NF-κβ, this followed by upregulation of anti-apoptotic genes BCL-2 and BCL-XL. AKT equally phosphorylates XIAP, which inhibits pro-apoptotic caspases like 3/7/9. It equally activates mTOR kinase, which phosphorylates mcl-1 an anti-apoptotic protein. Furthermore, activation of AKT leads to inhibition of pro-apoptotic proteins Bad, Bax, Bim and Noxa. Finally, phosphorylation of AKT inhibits FOXO3a thereby blocking pro-apoptotic protein of Bim and Noxa. Adapted from *Ashley et al.; 2014.*

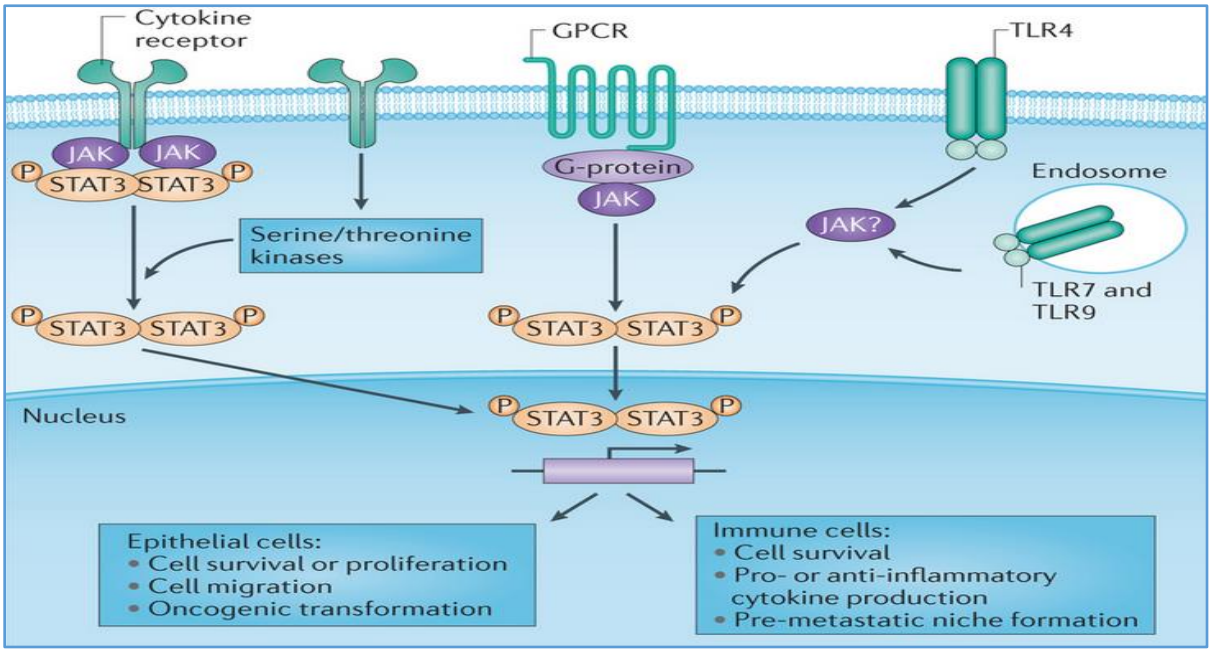

Supplementary Figure 4: **Radiation activation of JAK/STAT signaling pathway:** This activation of JAK/STAT pathway leads to transfer to the nucleus to promote transcription. This enhanced cell survival, proliferation, migration and oncogenic transformation.

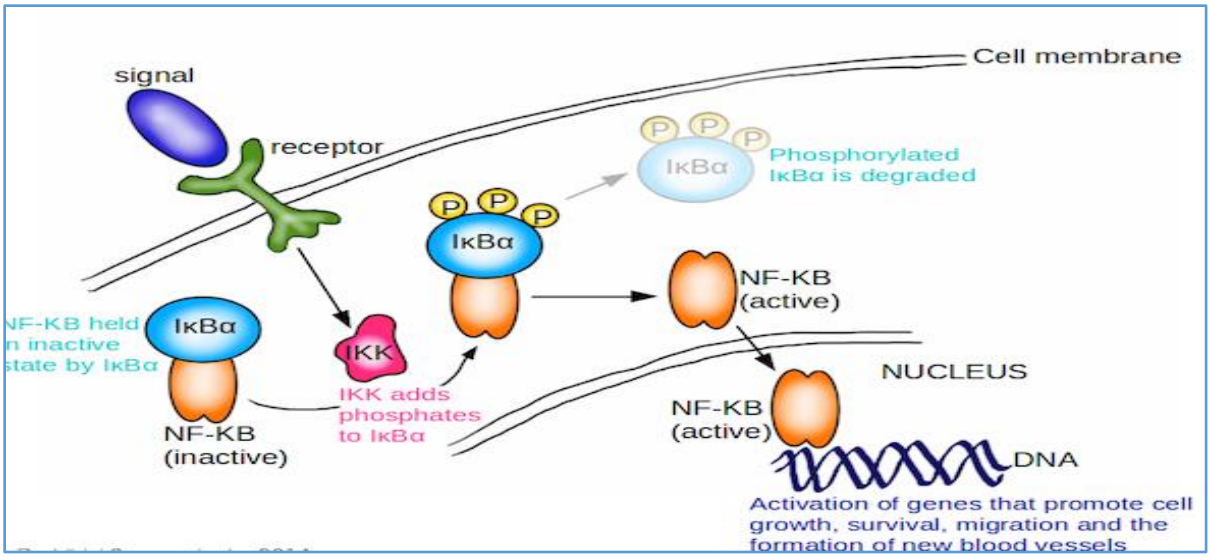

Supplementary figure 5: Radiation-induced NF-κβ signaling. IR activates NF-κβ is associated with transcription of vital genes in cell gowth, survival, proliferation and migration

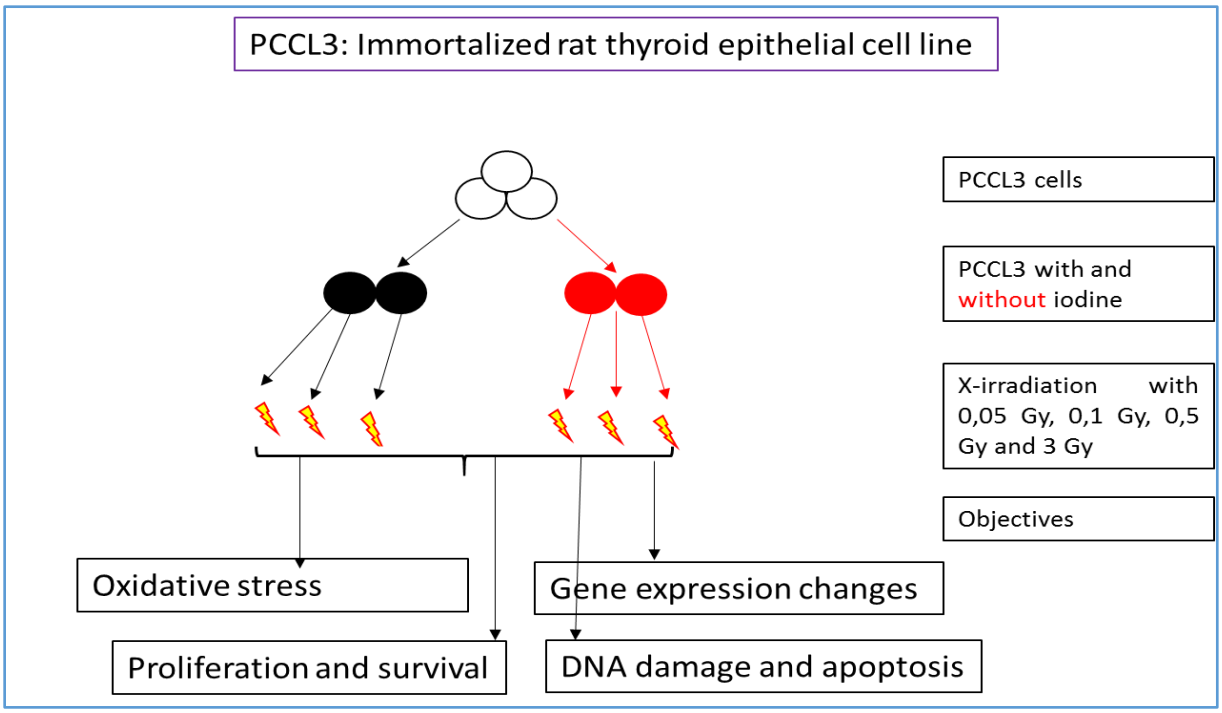

Supplementary Figure 6: Experimental Design

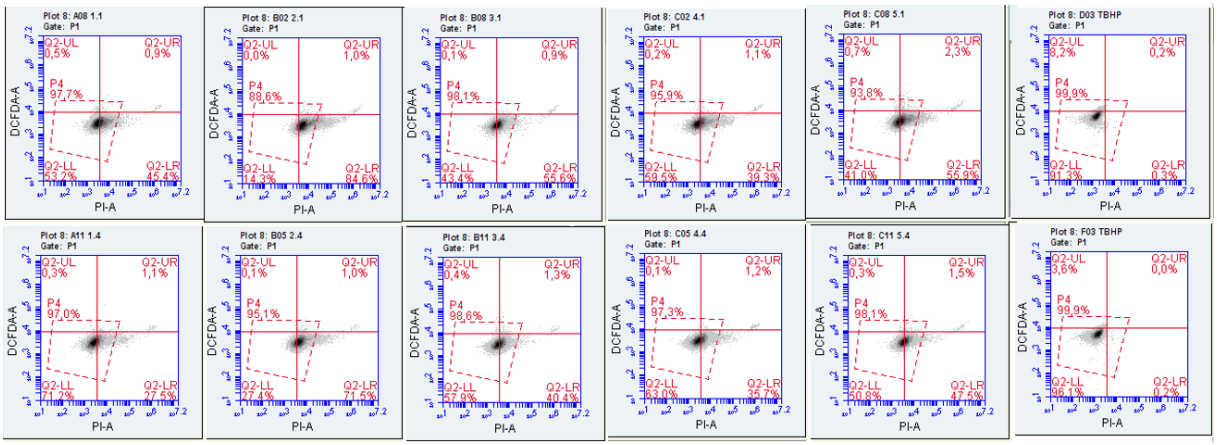

Supplementary figure 7: ROS detection with CM-H2DCFDA probe. A)The majority of the cells were positive for PI indicating (lower quadrants) while DCFDA positive cells (upper left quadrant) were barely detected (values range from 0.3-0.7%) at the control. Hence, the results could not be analyzed.

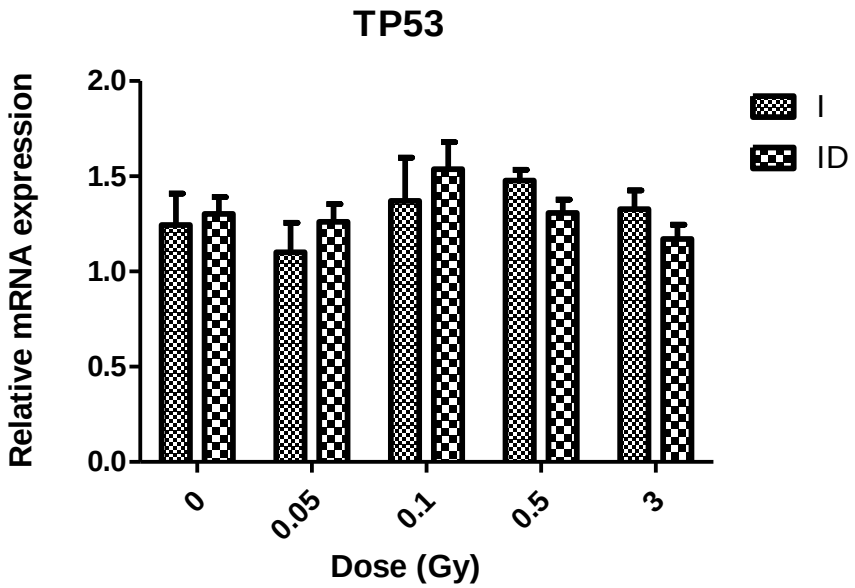

Supplementary figure 8: IR and ID had no significant effect on TP53 mRNA expression 24 hours following co-treatment (p< P=0.4203). There is no dose-dependent or additive effect on TP53 expression. mRNA expression was analyzed by RT-qPCR after PCCL3 cells were cultured 24 hours without iodine and exposed to low, intermediate and high radiation doses. Results are expressed as mean fold change ± standard deviation (SD) and normalized by β-actin.

Auteursrechtelijke overeenkomst

Ik/wij verlenen het wereldwijde auteursrecht voor de ingediende eindverhandeling:
Investigation of the biological effects of ionizing radiation and iodine deficiency on non-cancerous thyrocytes

Richting: **Master of Biomedical Sciences-Clinical Molecular Sciences**
Jaar: **2017**

in alle mogelijke mediaformaten, - bestaande en in de toekomst te ontwikkelen - , aan de Universiteit Hasselt.

Niet tegenstaand deze toekenning van het auteursrecht aan de Universiteit Hasselt behoud ik als auteur het recht om de eindverhandeling, - in zijn geheel of gedeeltelijk -, vrij te reproduceren, (her)publiceren of distribueren zonder de toelating te moeten verkrijgen van de Universiteit Hasselt.

Ik bevestig dat de eindverhandeling mijn origineel werk is, en dat ik het recht heb om de rechten te verlenen die in deze overeenkomst worden beschreven. Ik verklaar tevens dat de eindverhandeling, naar mijn weten, het auteursrecht van anderen niet overtreedt.

Ik verklaar tevens dat ik voor het materiaal in de eindverhandeling dat beschermd wordt door het auteursrecht, de nodige toelatingen heb verkregen zodat ik deze ook aan de Universiteit Hasselt kan overdragen en dat dit duidelijk in de tekst en inhoud van de eindverhandeling werd genotificeerd.

Universiteit Hasselt zal mij als auteur(s) van de eindverhandeling identificeren en zal geen wijzigingen aanbrengen aan de eindverhandeling, uitgezonderd deze toegelaten door deze overeenkomst.

Voor akkoord,

Nyuykonge, Bertrand

Datum: **8/06/2017**